11. Repeat step 7.
12. Develop the colour with appropriate chromogenic substrates (e.g. TMB microwell peroxidase substrate system [KPL, Gaithersburg, MD]) and read the absorbance.
13. Calculate the concentrations of samples by reference to the liner portion of the standard curve.

C. Cytokine-Specific ELISPOT

Like cytokine ELISA assay, several ELISPOT kits are commercially available. Thus, we summarize here a basic protocol of cytokine ELISPOT assay.

1. Dilute the capture antibody in PBS and add 100 μl to the wells of 96-well nitrocellulose-backed microtitre plate (e.g. Millititer-HA [Millipore, Billerica, MA]). Place the plates in a humidified chamber or carefully wrap the plate in saran wrap and incubate overnight at 4°C.
2. Remove the antibody solution from wells and block the immobilized antibody with culture medium (e.g. RPMI1640 medium containing 10% FCS) for 1 h at 37°C.
3. Rinse the plate three times with PBS.
4. Prepare the five-fold dilutions of purified T cells in culture medium starting at $1–10\times10^6$ cells/ml. Immediately add 100 μl of cells and incubate them for 12–16 h at 37°C. The time required for T cell purification significantly reduces the numbers of detectable cytokine-producing cells. Therefore, it is important to prepare the cells in a prompt manner.

   For the assessment of cytokine productions by antigen-specific T cells, purified T cells should be re-stimulated with the same antigens in the presence of irradiated antigen-presenting cells. Between 1 and 6 days after antigen stimulation, T cells are harvested and immediately added to the capture antibody-coated plates as described above.
5. Wash the plates three times with PBS followed by three times washes with PBS-T.
6. Add 100 μl of appropriate biotinylated capture antibody diluted in PBS-T with 1% BSA. Incubate the plates overnight at 4°C.
7. Wash the plates six times with PBS-T.
8. Add 100 μl of peroxidase-labelled anti-biotin antibody and incubate the plates for 1 h at room temperature.
9. Wash the plates four times with PBS.
10. Develop the colour with appropriate chromogenic substrates (e.g. AEC [BD Biosciences]) and count red spots by stereomicroscope or automated ELISPOT readers (e.g. KS ELISPOT [Carl Zeiss, Oberkochen, Germany]).

D. Intracellular Cytokine Staining

Using intracellular cytokine staining method, the frequency of cytokine-producing cells and their phenotypes can be determined by flow cytometer. By using subset-

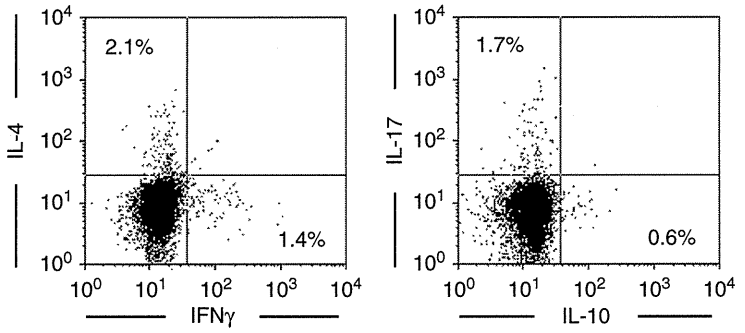

Figure 7. Intracellular cytokine staining of small intestinal T cells. Lymphocytes were isolated from the small intestine and cultured with 50 ng/ml PMA, 5 μM calcium ionophore A23187 and golgistop (BD Biosciences) for 4 h at 37°C. Cells were stained with anti-CD3 antibody followed by the fixation and permeabilization of cell membrane by Cytofix/Cytoperm kit (BD Biosciences). The permeable cells were further stained with antibodies specific for each cytokine and analysed by flow cytometry.

specific antibody, we do not need to purify the T cells. As example, we show here the data on cytokine-producing $CD4^+$ T cells isolated from small intestines (Figure 7).

1. Incubate lymphocytes in culture medium with 50 ng/ml PMA, 5 μM calcium ionophore A23187 and golgistop (BD Biosciences) for 4 h at 37°C.
2. Harvest the cells and stain cells with a corresponding cocktail of fluorescently labelled antibodies for 30 min at 4°C.
3. Wash the cells twice with PBS plus 2% FCS (PBS-F).
4. Fix the stained cells with 250 μl of Cytofix/Cytoperm solution (BD Biosciences) or 2% paraformaldehyde for 20 min at 4°C.
5. Wash cells twice with 1 ml of Perm/Wash buffer (BD Biosciences).
6. Incubate cells with fluorescently labelled cytokine-specific antibodies for 20 min at 4°C.
7. Repeat step 5 and suspend cells with PBS-T.
8. Analyse with Flow cytometer.

♦♦♦♦♦♦ IV. CONCLUSION

In this chapter, we have described the protocol for the analysis of T cell population in the intestine and their cytokine productions. For the cytokine production assay, we show three different methods: ELISA, ELISPOT and intracellular cytokine staining. These three assay systems allow the detection of different stages of cytokine production. Although each assay has unique advantages for the detection of T cell cytokines, the use of individual assays in a separate manner may often not

be sufficient for a thorough and accurate determination of the T cell cytokine profiles. Additionally, recent advances in the imaging technologies allow us to observe the cytokine-producing cells *in vivo* (Kamanaka *et al.*, 2006). Thus, combining traditional technologies with the modern and novel technologies will lead to the better understanding of T cell responses in the intestine.

Acknowledgements

This work was supported by grants from the Ministry of Education, Science, Sports, and Culture of Japan; the Ministry of Health and Welfare of Japan; the Global Center of Excellence (COE) program on Center of Education and Research for the Advanced Genome-based Medicine; and Yakult Bio-Science Foundation.

References

Asseman, C. and Powrie, F. (1998). Interleukin 10 is a growth factor for a population of regulatory T cells. *Gut* **42**, 157–158.

Beagley, K. W., Eldridge, J. H., Kiyono, H., Everson, M. P., Koopman, W. J., Honjo, T. and McGhee, J. R. (1988). Recombinant murine IL-5 induces high rate IgA synthesis in cycling IgA-positive Peyer's patch B cells. *J. Immunol.* **141**, 2035–2042.

Beagley, K. W., Eldridge, J. H., Lee, F., Kiyono, H., Everson, M. P., Koopman, W. J., Hirano, T., Kishimoto, T. and McGhee, J. R. (1989). Interleukins and IgA synthesis. Human and murine interleukin 6 induce high rate IgA secretion in IgA-committed B cells. *J. Exp. Med.* **169**, 2133–2148.

Bettelli, E., Carrier, Y., Gao, W., Korn, T., Strom, T. B., Oukka, M., Weiner, H. L. and Kuchroo, V. K. (2006). Reciprocal developmental pathways for the generation of pathogenic effector TH17 and regulatory T cells. *Nature* **441**, 235–238.

Chen, W., Jin, W., Hardegen, N., Lei, K. J., Li, L., Marinos, N., McGrady, G. and Wahl, S. M. (2003). Conversion of peripheral $CD4^{+}CD25^{-}$ naive T cells to CD4+CD25+ regulatory T cells by TGFβ induction of transcription factor Foxp3. *J. Exp. Med.* **198**, 1875–1886.

Coffman, R. L., Shrader, B., Carty, J., Mosmann, T. R. and Bond, M. W. (1987). A mouse T cell product that preferentially enhances IgA production. I. Biologic characterization. *J. Immunol.* **139**, 3685–3690.

Czerkinsky, C., Andersson, G., Ekre, H. P., Nilsson, L. A., Klareskog, L. and Ouchterlony, O. (1988). Reverse ELISPOT assay for clonal analysis of cytokine production. I. Enumeration of gamma-interferon-secreting cells. *J. Immunol. Methods* **110**, 29–36.

Groux, H., O'Garra, A., Bigler, M., Rouleau, M., Antonenko, S., de Vries, J. E. and Roncarolo, M. G. (1997). A $CD4^{+}$ T-cell subset inhibits antigen-specific T-cell responses and prevents colitis. *Nature* **389**, 737–742.

Hand, T. and Belkaid, Y. (2010). Microbial control of regulatory and effector T cell responses in the gut. *Curr. Opin. Immunol.* **22**, 63–72.

Harriman, G. R., Kunimoto, D. Y., Elliott, J. F., Paetkau, V. and Strober, W. (1988). The role of IL-5 in IgA B cell differentiation. *J. Immunol.* **140**, 3033–3039.

Harrington, L. E., Hatton, R. D., Mangan, P. R., Turner, H., Murphy, T. L., Murphy, K. M. and Weaver, C. T. (2005). Interleukin 17-producing $CD4^{+}$ effector T cells develop via a lineage distinct from the T helper type 1 and 2 lineages. *Nat. Immunol.* **6**, 1123–1132.

Kamanaka, M., Kim, S. T., Wan, Y. Y., Sutterwala, F. S., Lara-Tejero, M., Galan, J. E., Harhaj, E. and Flavell, R. A. (2006). Expression of interleukin-10 in intestinal lymphocytes detected by an interleukin-10 reporter knockin tiger mouse. *Immunity* **25**, 941–952.

Kiyono, H., Kunisawa, J., McGhee, J. R. and Mestecky, J. (2008). The mucosal immune system. In: *Fundamental Immunology* (W. E. Paul, ed.), pp. 983–1030. Lippincott-Raven, Philadelphia.
Kunisawa, J., Nochi, T. and Kiyono, H. (2008). Immunological commonalities and distinctions between airway and digestive immunity. *Trends Immunol.* **29**, 505–513.
Littman, D.R. and Rudensky, A.Y. (2010). Th17 and regulatory T cells in mediating and restraining inflammation. *Cell* **140**, 845–858.
Mosmann, T. R. and Coffman, R. L. (1989). Th1 and Th2 cells: different patterns of lymphokine secretion lead to different functional properties. *Annu. Rev. Immunol.* **7**, 145–173.
Sakaguchi, S., Yamaguchi, T., Nomura, T. and Ono, M. (2008). Regulatory T cells and immune tolerance. *Cell* **133**, 775–787.
Seder, R. A. and Paul, W. E. (1994). Acquisition of lymphokine-producing phenotype by CD4+ T cells. *Annu. Rev. Immunol.* **12**, 635–673.
Street, N. E. and Mosmann, T. R. (1991). Functional diversity of T lymphocytes due to secretion of different cytokine patterns. *FASEB J.* **5**, 171–177.
Stumhofer, J. S., Silver, J. S., Laurence, A., Porrett, P. M., Harris, T. H., Turka, L. A., Ernst, M., Saris, C. J., O'Shea, J. J. and Hunter, C. A. (2007). Interleukins 27 and 6 induce STAT3-mediated T cell production of interleukin 10. *Nat. Immunol.* **8**, 1363–1371.
Weaver, C. T., Hatton, R. D., Mangan, P. R. and Harrington, L. E. (2007). IL-17 family cytokines and the expanding diversity of effector T cell lineages. *Annu. Rev. Immunol.* **25**, 821–852.
Zhou, L., Ivanov, I. I., Spolski, R., Min, R., Shenderov, K., Egawa, T., Levy, D. E., Leonard, W. J. and Littman, D. R. (2007). IL-6 programs Th17 cell differentiation by promoting sequential engagement of the IL-21 and IL-23 pathways. *Nat. Immunol.* **8**, 967–974.

Peaceful Mutualism in the Gut: Revealing Key Commensal Bacteria for the Creation and Maintenance of Immunological Homeostasis

Jun Kunisawa[1,2,*] and Hiroshi Kiyono[1,2,3]
[1]Division of Mucosal Immunology, Department of Microbiology and Immunology, The Institute of Medical Science
[2]Department of Medical Genome Science, Graduate School of Frontier Science
[3]Graduate School of Medicine
The University of Tokyo, Tokyo 108-8639, Japan
*Correspondence: kunisawa@ims.u-tokyo.ac.jp
DOI 10.1016/j.chom.2011.01.012

Quantitative and qualitative aspects of commensal bacteria determine the active and quiescent status of host immunity. In a recent *Science* paper, **Atarashi et al. (2011)** identify *Clostridium* clusters IV and XIVa as indigenous commensal bacteria that induce regulatory T cells for the creation and maintenance of immunological homeostasis.

The intestinal tract of mammals is home to 10^{13} to 10^{14} commensal bacteria composed of hundreds of species that benefit the host by supplying nutrients, metabolizing otherwise indigestible food, and preventing colonization by pathogens. Additionally, immune system development requires interactions with commensal bacteria (Hill and Artis, 2010). Because commensal bacteria commonly produce ligands of innate immunity, it was thought that unspecified commensal bacteria indiscriminately induced immune system development. However, accumulating evidence has indicated that individual species of commensal bacteria play specific roles in determining the immunological balance in the mucosal and systemic compartments. In a recent issue of *Science*, Honda and colleagues identified a cluster of indigenous commensal bacteria that are key to maintaining quiescent immunity (Atarashi et al., 2011).

Recent advances in genetic analyses of the composition of commensal bacteria led to the discovery that changes in microbial composition accompany alterations in the quality of host immunity and occasionally underlie immune diseases such as inflammatory bowel diseases (IBD) (Hill and Artis, 2010). These findings straightforwardly led to works addressing the puzzling question of how specific species of commensal bacteria regulate particular immune responses. One example of recent success in this area is the identification of segmented filamentous bacteria (SFB) as inducers of active immunity. Several groups, including Honda's, showed that SFB efficiently induce effector T cells, especially Th17 cells observed predominantly in the gut, where they provide protective immunity against intestinal infection (Gaboriau-Routhiau et al., 2009; Ivanov et al., 2009).

In addition to immunosurveillance against harmful pathogens, the gut immune system mediates quiescent immunity (or tolerance/unresponsiveness) against harmless and beneficial nonself materials such as dietary antigens and commensal bacteria. Among multiple immunoregulatory pathways, regulatory T (Treg) cells play pivotal roles in achieving quiescent immunity. Like Th17 cells, Treg cells are abundantly present in the gut, which is explained at least partly by the function of the vitamin A metabolite retinoic acid that is produced by gut-associated dendritic cells (Mucida et al., 2009). Although probiotic strains could also induce Treg cells in the gut (Kwon et al., 2010), whether and how indigenous commensal bacteria induce Treg cells remained unclear.

In their recent *Science* paper, Honda's group extends their studies and identifies *Clostridium* clusters IV and XIVa (also known as the *Clostridium leptum* and *coccoides groups*) as among the indigenous commensal bacteria inducing colonic Treg cells. Atarashi et al. (2011) demonstrated that only a few Treg cells were present in the colon of germ-free mice but increased to normal levels in specific pathogen-free (SPF) mice by colonization with commensal bacteria originating from SPF mice. By eliminating bacteria using antibiotics and chemical reagents, together with information about prominent commensal bacteria in the colon, they identified gram-positive and spore-forming *Clostridia* as candidate commensal bacteria that induce colonic Treg cells. Direct evidence was obtained from gnotobiotic mice that were generated by colonization with *Clostridium* clusters IV and XIVa. Intriguingly, the induction of Treg cells by commensal bacteria was observed specifically in the colon, whereas Treg cells in the small intestine were normally present in germ-free mice (Atarashi et al., 2011). The physiological functions of the small and large intestines differ substantially, and the small intestine is specialized to digest and absorb dietary materials. Treg cells in the small intestine increase after weaning (Atarashi et al., 2011), raising the possibility that materials in the diet and/or breast milk may regulate the induction of Treg cells in the small intestine.

Atarashi et al. also showed that an artificial increase in *Clostridium* in neonatal SPF mice resulted in the attenuation of intestinal inflammation in adulthood, which is potentially related to the lower levels of *Clostridium* clusters IV and XIVa in IBD patients (Frank et al., 2007). These regulatory effects were mediated by the preferential induction of Treg cells that produced IL-10 and expressed high levels of cytotoxic T-lymphocyte antigen

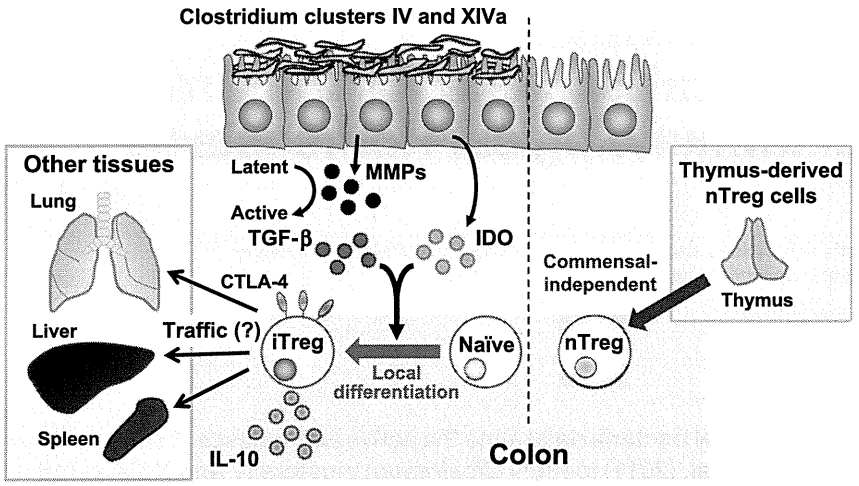

Figure 1. Induction of IL-10-Producing-Induced Treg (iTreg) Cells through the Interaction between Indigenous *Clostridium* Species and Epithelial Cells
After weaning, *Clostridium* clusters IV and XIVa become prominent in the colon, where they form a thick layer on the epithelium. *Clostridium* clusters IV and XIVa promote the production of matrix metalloproteinases (MMPs) from epithelial cells to convert TGF-β from the latent to the active form. Together with indoleamine 2,3-dioxygenase (IDO) produced by epithelial cells, the active form of TGF-β converts non-Treg cells into induced Treg (iTreg) cells that produce IL-10 and express high levels of CTLA-4. The locally differentiated iTreg cells prevent inflammatory and allergic responses in the gut and presumably other remote tissues. In contrast, thymus-derived naturally occurring Treg (nTreg) cells do not require stimulation by commensal bacteria.

4 (CTLA-4) (Figure 1). Interestingly, colonization with *Clostridium* resulted in the specific increase of IL-10-producing Treg cells at distant tissues, such as the spleen and lung, and inhibited allergic responses. These data suggest that T cells educated by commensal bacteria may move from the gut to remote tissues, where they determine the T cell-mediated immunological balance. This idea is plausible based on recent findings that Th17 cells induced by gut-resident SFB have pathogenic roles in the development of arthritis (Wu et al., 2010) and that probiotic-induced Treg cells accumulate at inflammatory sites of various tissues (Kwon et al., 2010).

Investigating the mechanisms of *Clostridium*-mediated induction of Treg cells, Atarashi et al. showed that *Clostridium* formed a thick colonizing layer on the epithelium where it enhanced the release of the active form of TGF-β and indoleamine 2,3-dioxygenase (IDO) from epithelial cells (Atarashi et al., 2011) (Figure 1). The TGF-β pathway was mediated by increasing the gene transcription of matrix metalloproteinases that converted latent TGF-β into the active form. Therefore, colonization with *Clostridium* preferentially converts non-Treg cells into Helios-negative induced Treg cells with little effect on Helios-positive thymus-derived naturally occurring Treg cells. A recent study demonstrated that a mixture of probiotic strains, including *Lactobacillus* and *Bifidobacterium*, enhanced the production of TGF-β and IDO from dendritic cells and consequently induced Treg cells (Kwon et al., 2010), similar to the effects of *Clostridium* on epithelial cells. Interestingly, Atarashi et al. (2011) demonstrated that colonization with a mixture of three *Lactobacillus* strains was not sufficient to induce colonic Treg cells, suggesting that the generation of a bacterial community in which bacteria respond to each other's metabolic products and establish a niche among commensals is important to create an environment that facilitates the induction of Treg cells. Another major unresolved question is the function of *Clostridium* in the induction of colonic Treg cells. Atarashi et al. mention that pattern-recognition receptors were not involved in this pathway, in contrast to the Toll-like receptor 2-dependent conversion of Treg cells induced by polysaccharide A by the human commensal *Bacteroides fragilis* (Round and Mazmanian, 2010). Collectively, these findings suggest that there are versatile pathways in the commensal bacteria-mediated induction of Treg cells, and thus it is important to examine not only bacteria-host interactions but also the role of the bacterial community in the establishment of immunological mutualism. The role of dietary materials (e.g., fatty acids, vitamins, and carbohydrates) in the three-way communications with the host and commensal bacteria is an additional fascinating subject (Maslowski and Mackay, 2011). These future studies will facilitate our understanding of how our immune system mutually evolves with commensal bacteria to achieve the protective but still homeostatic immunity in the intricate environment of the gut, and will also lead to novel strategies to prevent and treat inflammatory, allergic, and infectious diseases.

REFERENCES

Atarashi, K., Tanoue, T., Shima, T., Imaoka, A., Kuwahara, T., Momose, Y., Cheng, G., Yamasaki, S., Saito, T., Ohba, Y., et al. (2011). Science *331*, 337–341.

Frank, D.N., St Amand, A.L., Feldman, R.A., Boedeker, E.C., Harpaz, N., and Pace, N.R. (2007). Proc. Natl. Acad. Sci. USA *104*, 13780–13785.

Gaboriau-Routhiau, V., Rakotobe, S., Lecuyer, E., Mulder, I., Lan, A., Bridonneau, C., Rochet, V., Pisi, A., De Paepe, M., Brandi, G., et al. (2009). Immunity *31*, 677–689.

Hill, D.A., and Artis, D. (2010). Annu. Rev. Immunol. *28*, 623–667.

Ivanov, I.I., Atarashi, K., Manel, N., Brodie, E.L., Shima, T., Karaoz, U., Wei, D., Goldfarb, K.C., Santee, C.A., Lynch, S.V., et al. (2009). Cell *139*, 485–498.

Kwon, H.K., Lee, C.G., So, J.S., Chae, C.S., Hwang, J.S., Sahoo, A., Nam, J.H., Rhee, J.H., Hwang, K.C., and Im, S.H. (2010). Proc. Natl. Acad. Sci. USA *107*, 2159–2164.

Maslowski, K.M., and Mackay, C.R. (2011). Nat. Immunol. *12*, 5–9.

Mucida, D., Park, Y., and Cheroutre, H. (2009). Semin. Immunol. *21*, 14–21.

Round, J.L., and Mazmanian, S.K. (2010). Proc. Natl. Acad. Sci. USA *107*, 12204–12209.

Wu, H.J., Ivanov, I.I., Darce, J., Hattori, K., Shima, T., Umesaki, Y., Littman, D.R., Benoist, C., and Mathis, D. (2010). Immunity *32*, 815–827.

The Airway Antigen Sampling System: Respiratory M Cells as an Alternative Gateway for Inhaled Antigens

Dong-Young Kim,*,†,[1] Ayuko Sato,*,[1] Satoshi Fukuyama,*,[1] Hiroshi Sagara,‡ Takahiro Nagatake,*,§ Il Gyu Kong,*,†,§ Kaoru Goda,* Tomonori Nochi,* Jun Kunisawa,*,¶ Shintaro Sato,* Yoshifumi Yokota,‖ Chul Hee Lee,† and Hiroshi Kiyono*,§,¶,#,**

In this study, we demonstrated a new airway Ag sampling site by analyzing tissue sections of the murine nasal passages. We revealed the presence of respiratory M cells, which had the ability to take up OVA and recombinant *Salmonella typhimurium* expressing GFP, in the turbinates covered with single-layer epithelium. These M cells were also capable of taking up respiratory pathogen group A *Streptococcus* after nasal challenge. Inhibitor of DNA binding/differentiation 2 (Id2)-deficient mice, which are deficient in lymphoid tissues, including nasopharynx-associated lymphoid tissue, had a similar frequency of M cell clusters in their nasal epithelia to that of their littermates, $Id2^{+/-}$ mice. The titers of Ag-specific Abs were as high in $Id2^{-/-}$ mice as in $Id2^{+/-}$ mice after nasal immunization with recombinant *Salmonella*-ToxC or group A *Streptococcus*, indicating that respiratory M cells were capable of sampling inhaled bacterial Ag to initiate an Ag-specific immune response. Taken together, these findings suggest that respiratory M cells act as a nasopharynx-associated lymphoid tissue-independent alternative gateway for Ag sampling and subsequent induction of Ag-specific immune responses in the upper respiratory tract. *The Journal of Immunology*, **2011, 186: 4253–4262.**

The initiation of Ag-specific immune responses occurs at special gateways, M cells, which are located in the epithelium overlying MALT follicles such as nasopharynx-associated lymphoid tissue (NALT) and Peyer's patches (1). Peyer's patches contain all of the immunocompetent cells that are required for the generation of an immune response and are the key inductive tissues for the mucosal immune system. Peyer's patches are interconnected with effector tissues (e.g., the lamina propria of the intestine) for the induction of IgA immune responses specific to ingested Ags (2). NALT also contains all of the necessary lymphoid cells, including T cells, B cells, and APCs, for the induction and regulation of inhaled Ag-specific mucosal immune responses (1, 3). This tissue is rich in Th0-type $CD4^+$ T cells, which can become either Th1- or Th2-type cells (4). NALT is also equipped with the molecular and cellular environments for class-switch recombination of μ to α genes for the generation of IgA-committed B cells and the induction of memory B cells (5, 6). It is thus widely accepted that NALT M cells are key players in the uptake of nasally delivered Ags for the subsequent induction of Ag-specific IgA immune responses (1). As a result, NALT is considered a potent target for mucosal vaccines (1).

A recent study identified NALT-like structures of lymphocyte aggregates with follicle formation in the human nasal mucosa, especially in the middle turbinate of children <2 y old (7). Another recent study showed that, postinfection of mice with influenza via the upper respiratory tract, the levels of Ag-specific Ig observed in the serum and in nasal mucosal secretions after surgical removal of NALT were comparable to those in tissue-intact mice (8). Other studies have demonstrated that Ag-specific immune responses are induced in lymphotoxin-$\alpha^{-/-}$ and $CXCL13^{-/-}$ mice, in which the NALT exhibits structural and functional defects (9, 10). Thus, despite the central role of NALT in the generation of Ag-specific Th cells and IgA-committed B cells against inhaled Ags, these tissues do not appear essential for the induction of Ag-specific immune responses, suggesting that additional inductive sites and/or M cells are present in the upper respiratory tract.

The major goal of our study was to search for an NALT-independent M cell-operated gateway by examining and characterizing the entire nasal mucosa. We were able to identify M cells developed in the murine nasal passage epithelium as an alternative and NALT-independent gateway for the sampling of respiratory Ags and the subsequent induction of Ag-specific immune

*Division of Mucosal Immunology, Department of Microbiology and Immunology, Institute of Medical Science, University of Tokyo, Tokyo 108-8639, Japan; †Department of Otorhinolaryngology, Seoul National University College of Medicine, Seoul 110-744, Korea; ‡Medical Proteomics Laboratory, Institute of Medical Science, University of Tokyo, Tokyo 108-8639, Japan; §Graduate School of Medicine and Faculty of Medicine, University of Tokyo, Tokyo 113-0033, Japan; ¶Graduate School of Frontier Sciences, University of Tokyo, Chiba 277-8561, Japan; ‖Department of Molecular Genetics, School of Medicine, University of Fukui, Fukui 910-1193, Japan; #Immunobiology Vaccine Center, University of Alabama at Birmingham, Birmingham, AL 35294; and **Department of Pediatric Dentistry, University of Alabama at Birmingham, Birmingham, AL 35294

[1]D.-Y.K., A.S., and S.F contributed equally to this work.

Received for publication November 25, 2009. Accepted for publication February 2, 2011.

This work was supported by grants-in-aid from the Ministry of Education, Science, Sports, and Culture and the Ministry of Health and Welfare of Japan. Part of the study was also supported by grants from the Joint Research Project under the Korea–Japan Basic Scientific Cooperation Program for FY 2007, Seoul National University Hospital Research Fund 05-2007-004, and the Waksman Foundation. D.-Y.K. was supported by research fellowships from the Japan Society for the Promotion of Science for Foreign Researchers. S.F., T.N., and T.N. were supported by research fellowships from the Japan Society for the Promotion of Science for Young Scientists.

Address correspondence and reprint requests to Dr. Hiroshi Kiyono, Division of Mucosal Immunology, Department of Microbiology and Immunology, Institute of Medical Science, University of Tokyo, 4-6-1 Shirokanedai, Minato-ku, Tokyo 108-8639, Japan. E-mail address: kiyono@ims.u-tokyo.ac.jp

The online version of this article contains supplemental material.

Abbreviations used in this article: DC, dendritic cell; dLN, draining lymph node; GAS, group A *Streptococcus*; GFP-*Salmonella*, GFP-expressing *Salmonella*; Id2, inhibitor of DNA binding/differentiation 2; NALT, nasopharynx-associated lymphoid tissue; *Salmonella*-GFP, *Salmonella typhimurium* expressing GFP; SEM, scanning electron microscopy; TEM, transmission electron microscopy; TT, tetanus toxoid; UEA-1, *Ulex europaeus* agglutinin-1; WGA, wheat germ agglutinin.

www.jimmunol.org/cgi/doi/10.4049/jimmunol.0903794

responses. Characterization of respiratory M cells should accelerate our understanding of the Ag sampling system at work in the upper respiratory tract.

Materials and Methods

Mice

BALB/c mice were purchased from SLC (Shizuoka, Japan). Inhibitor of DNA binding/differentiation 2 $(Id2)^{-/-}$ mice (129/Sv), generated as previously described (11), were maintained together with their littermate $Id2^{+/-}$ mice in a specific pathogen-free environment at the experimental animal facility of the Institute of Medical Science, University of Tokyo. All experiments were carried out according to the guidelines provided by the Animal Care and Use Committees of the University of Tokyo.

M cell staining

For the preparation of nasal cavity samples for confocal microscopy, we decapitated euthanized mice and then, with their heads immobilized, removed the lower jaw together with the tongue. Using the hard palate as a guide, we then used a large scalpel to remove the snout with a transverse cut behind the back molars. After removing the skin and any excess soft tissue, we flushed the external nares with PBS to wash out any blood within the nasal cavity before freezing the nasal passage tissue in Tissue-Tek OCT embedding medium (Miles, Elkhart, IN) in a Tissue-Tek Cryomold. For immunofluorescence staining, we prepared 5-μm–thick frozen sections by using a CryoJane Tape-Transfer System (Instrumedics, St. Louis, MO), allowed the sections to air dry, and then fixed them in acetone at 4°C. We then rehydrated the sections in PBS and incubated them for a further 30 min in Fc blocking solution. For M cell staining, sections were incubated overnight with rhodamine-labeled *Ulex europaeus* agglutinin-1 (UEA-1; Vector Laboratories, Burlingame, CA) at a concentration of 20 μg/ml and FITC-labeled M cell-specific mAb NKM 16-2-4 (12) at 5 μg/ml or FITC-labeled wheat germ agglutinin (WGA; Vector Laboratories, Burlingame, CA) at 10 μg/ml and counterstained with DAPI (Molecular Probes, Eugene, OR) at 0.2 μg/ml in PBS (13).

Electron microscopic analysis of respiratory M cells

For electron microscopic analysis, the nasal cavity sample was prepared and vigorously washed as described above, and then fixed on ice for 1 h in a solution containing 0.5% glutaraldehyde, 4% paraformaldehyde, and 0.1 M sodium phosphate buffer (pH 7.6). After being washed with 4% sucrose in 0.1 M phosphate buffer, the tissues were incubated in an HRP-conjugated UEA-1 solution (20 μg/ml) for 1 h at room temperature. The peroxidase reaction was developed by incubating the tissues for 10 min at room temperature with 0.02% 3,3′-diaminobenzidine tetrahydrochloride in 0.05 M Tris-HCl (pH 8) containing 0.01% H_2O_2. After being washed with the same buffer, the tissues were fixed again with 2.5% glutaraldehyde in 0.1 M phosphate buffer overnight. The nasal passage tissue was decalcified with 2.5% EDTA solution for 5 d. After being washed three times with the same buffer, samples were fixed with 2% osmium tetraoxide on ice for 1 h before being dehydrated with a series of ethanol gradients. For scanning electron microscopy (SEM), dehydrated tissues were freeze-embedded in *t*-butyl alcohol and freeze-dried, then coated with osmium and observed with a Hitachi S-4200 scanning electron microscope (Hitachi, Tokyo, Japan). For transmission electron microscopy (TEM) analysis, the samples were embedded in Epon 812 Resin mixture (TAAB Laboratories Equipment, Berks, U.K.), and ultrathin (70-nm) sections were cut with a Reichert Ultracut N Ultramicrotome (Leica Microsystems, Heidelberg, Germany). Ultrathin sections were stained with 2% uranyl acetate in 70% ethanol for 5 min at room temperature and then in Reynolds lead citrate for 5 min at room temperature. Sections were examined with a Hitachi H-7500 transmission electron microscope (Hitachi, Tokyo, Japan).

Elucidation of M cell numbers

To examine the numbers of respiratory and NALT M cells, mononuclear cells (including M cells, epithelial cells, and lymphocytes) were isolated from the nasal passages and NALT as previously described, with some modifications (4). In brief, the palatine plate containing NALT was removed, and then NALT was dissected out. Nasal passage tissues without NALT were also extracted from the nasal cavity, and mononuclear cells from individual tissues were isolated by gentle teasing using needles through 40-μm nylon mesh. The total numbers of cells isolated from the two preparations were counted. These single-cell preparations were then labeled with PE–UEA-1 (Biogenesis, Poole, England), and the percentages of UEA-1–positive epithelial cells in the nasal passages and NALT were determined with a flow cytometer (FACSCalibur; BD Biosciences, Franklin Lakes, NJ). The numbers of M cells and goblet cells in the nasal passages and NALT were counted by confocal microscopic analysis according to the patterns of staining with UEA-1 and WGA. That is, the frequencies of M cells ($UEA\text{-}1^{+}WGA^{-}$) and goblet cells ($UEA\text{-}1^{+}WGA^{+}$) were determined by the enumeration of each type in 100 $UEA\text{-}1^{+}$ cells. The formula used to estimate the number of M cells was: [(total number of mononuclear cells × percentage of $UEA\text{-}1^{+}$ epithelial cells) × M cells/$UEA\text{-}1^{+}$ epithelial cells]. The number of respiratory M cells in $Id2^{-/-}$ mice was calculated in the same manner.

Ag uptake in situ

DQ OVA was purchased from Molecular Probes. *Salmonella typhimurium* PhoPc strain transformed with the pKKGFP plasmid was kindly provided by F. Niedergang (14, 15). Group A *Streptococcus* (GAS; *Streptococcus pyogenes* ATCC BAA-1064) was obtained from the American Type Culture Collection (Manassas, VA), and immunofluorescence staining with FITC-conjugated goat anti-*Streptococcus* A Ab (Cortex Biochem, San Leandro, CA) was used to detect GAS uptake. DQ OVA (0.5 mg), GFP-expressing *Salmonella* (GFP-*Salmonella*) (5×10^8 CFU), or GAS (5×10^8 CFU) was intranasally administered and incubated in situ. Thirty minutes after the intranasal administration, the nasal passages were removed as described above and extensively washed with cold PBS with antibiotic solution to remove weakly adherent and/or extracellular DQ OVA or bacteria, as described (13).

The airway fluorescence-labeled Ag-treated nasal passages were processed for confocal microscopy as described above or for FACSCalibur flow cytometric analysis as follows. Mononuclear cells (including M cells, epithelial cells, and lymphocytes) were physically isolated from the nasal passages and NALT as described above, fixed in 4% paraformaldehyde, and labeled with PE–UEA-1 (Biogenesis, Poole, England). The percentage of green fluorescence (BODYPI FL or GFP)/UEA-1 double-positive nasal passage epithelial cells was determined by using an FACSCalibur (BD Biosciences).

To clarify the uptake of the bacteria by M cells, $UEA\text{-}1^{+}GFP^{+}$ cells, which were sorted from the nasal passages of mice intranasally infected with GFP-*Salmonella* by using an FACSAria cell sorter (BD Biosciences) were analyzed under three-dimensional confocal microscopy (Leica Microsystems).

To demonstrate the presence of dendritic cells (DCs) in the submucosa of the nasal passages, especially underneath respiratory M cells, after intranasal instillation of GAS, we used FITC- or allophycocyanin-conjugated anti-mouse CD11c (BD Pharmingen, San Jose, CA) Abs for subsequent confocal microscopic analysis.

Immunization

The recombinant *S. typhimurium* BRD 847 strain used in this study was a double *aroA aroD* mutant that expressed the nontoxic, immunogenic 50-kDa ToxC fragment of tetanus toxin from the plasmid pTET*nir*15 under the control of the anaerobically inducible *nirB* promoter (recombinant *Salmonella*-ToxC) (16). As a control, recombinant *Salmonella* that did not express ToxC was used. The recombinant *Salmonella* organisms were resuspended in PBS to a concentration of 2.5×10^{10} CFU/ml. Bacterial suspensions were intranasally administered by pipette (10 μl/mouse) three times at weekly intervals. To eliminate any possible GALT-associated induction of Ag-specific immune responses from the swallowing of bacterial solutions after intranasal immunization, mice were given drinking water containing gentamicin from 1 wk before the immunization to the end of the experiment and were also subjected to intragastric lavage with 500 μl gentamicin solution before and after intranasal immunization. This protocol successfully eliminated the possibility of the intranasally delivered bacteria becoming deposition in the intestine (Supplemental Fig. 1). The titers of tetanus toxoid (TT)-specific serum IgG and mucosal IgA Abs were determined by end-point ELISA, as described previously (17).

To measure GAS-specific immune responses, GAS was suspended in PBS to a concentration of 2×10^{10} CFU/ml. Ten microliters bacterial suspension was intranasally administered once using a pipette. Six weeks after the administration, serum and nasal washes were prepared, and the titers of GAS-specific Ab were measured by ELISA using a previously described protocol (18).

Statistical analysis

Data are expressed as means ± SD, and the difference between groups was assessed by the Mann–Whitney *U* test. The p values <0.05 were considered to be statistically significant.

Results

Respiratory M cells in single-layer epithelium of the nasal passage

The nasal respiratory epithelium of the mouse is composed mainly of pseudostratified ciliated columnar epithelium (19). However, when H&E-stained sections of the whole nasal cavity were examined, a single-layer epithelium was found to cover some regions of the nasal cavity, especially the lateral surfaces of the nasal turbinates (Fig. 1*A–C*). Frozen sections of nasal passages from naive BALB/c mice were prepared and stained with FITC-WGA (green) and rhodamine–UEA-1 (red), and then counterstained with DAPI (blue). Clusters of UEA-1$^+$WGA$^-$ cells that shared M cell characteristics were found exclusively in the single-layer epithelium of the nasal passage covered by ciliated columnar epithelial cells (Fig. 1*D*, 1*E*). Some respiratory M cells were also occasionally found on the transitional area between the single-layer and stratified epithelium. Notably, respiratory M cells also reacted with our previously developed M cell-specific mAb NKM 16-2-4 (12), demonstrating colocalization of the signals of UEA-1 and NKM 16-2-4 (Fig. 1*F*, 1*G*).

Electron microscopic analysis of respiratory M cells

SEM of the respiratory M cells revealed the characteristic features of M cells: a depressed surface with short and irregular microvilli (Fig. 2*A*, 2*B*). TEM analysis revealed that the respiratory M cell was covered by shorter and more irregular microvilli (with definite UEA-1$^+$ signals; Fig. 2*C*, 2*D*) than were found in neighboring ciliated columnar respiratory epithelial cells (Fig. 2*E*). However, no pocket formation (or pocket lymphocytes) was seen in the basal membranes of respiratory M cells, unlike in NALT M cells (Fig. 2*F*, 2*G*). These findings indicated that the newly identified respiratory M cells had most of the unique morphological characteristics of classical M cells.

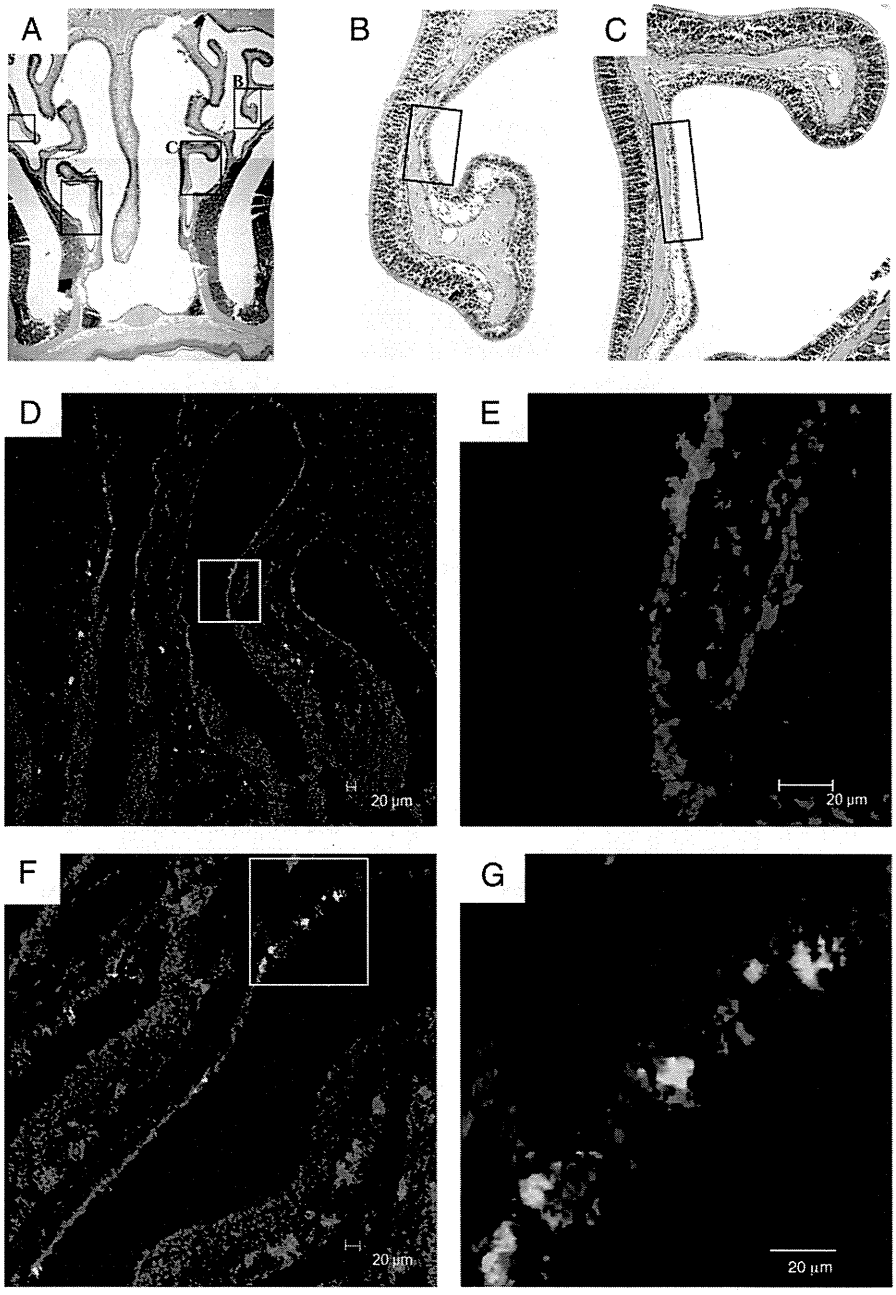

FIGURE 1. Clusters of UEA-1$^+$WGA$^-$ respiratory M cells are found selectively in the single-layer epithelium of the nasal passage. *A–C*, H&E staining reveals the anatomy and general histology of the murine nasal passage (*A*, original magnification ×40). The nasal respiratory epithelium of the mouse is covered with a pseudostratified ciliated columnar epithelium. However, a single-layer epithelium was found on the lateral surfaces of the nasal turbinates (*B*, *C*). Original magnification ×100. Rectangles indicate areas covered with the single-layer epithelium. The results are representative of three independent experiments. *D–G*, Confocal views of UEA-1$^+$ cells in the nasal epithelium of turbinates. Frozen sections were prepared and stained with FITC-WGA (green) and rhodamine–UEA-1 (red), and then counterstained with DAPI (blue) (*D*, *E*). Scale bars, 20 μm. The merged image is shown in *D*. An enlargement of the area in the rectangle in *D* is shown in *E*. UEA-1$^+$WGA$^-$ cells are clustered on the single-layer nasal epithelium of the turbinate. *F* and *G*, UEA-1$^+$ cells also reacted with our previously developed M cell-specific mAb NKM 16-2-4, demonstrating colocalization of signals of rhodamine–UEA-1 (red) and FITC-NKM 16-2-4 (green). The merged image is shown in *F*. An enlargement of an area from the rectangle in *F* is shown in *G*. The results are representative of five independent experiments.

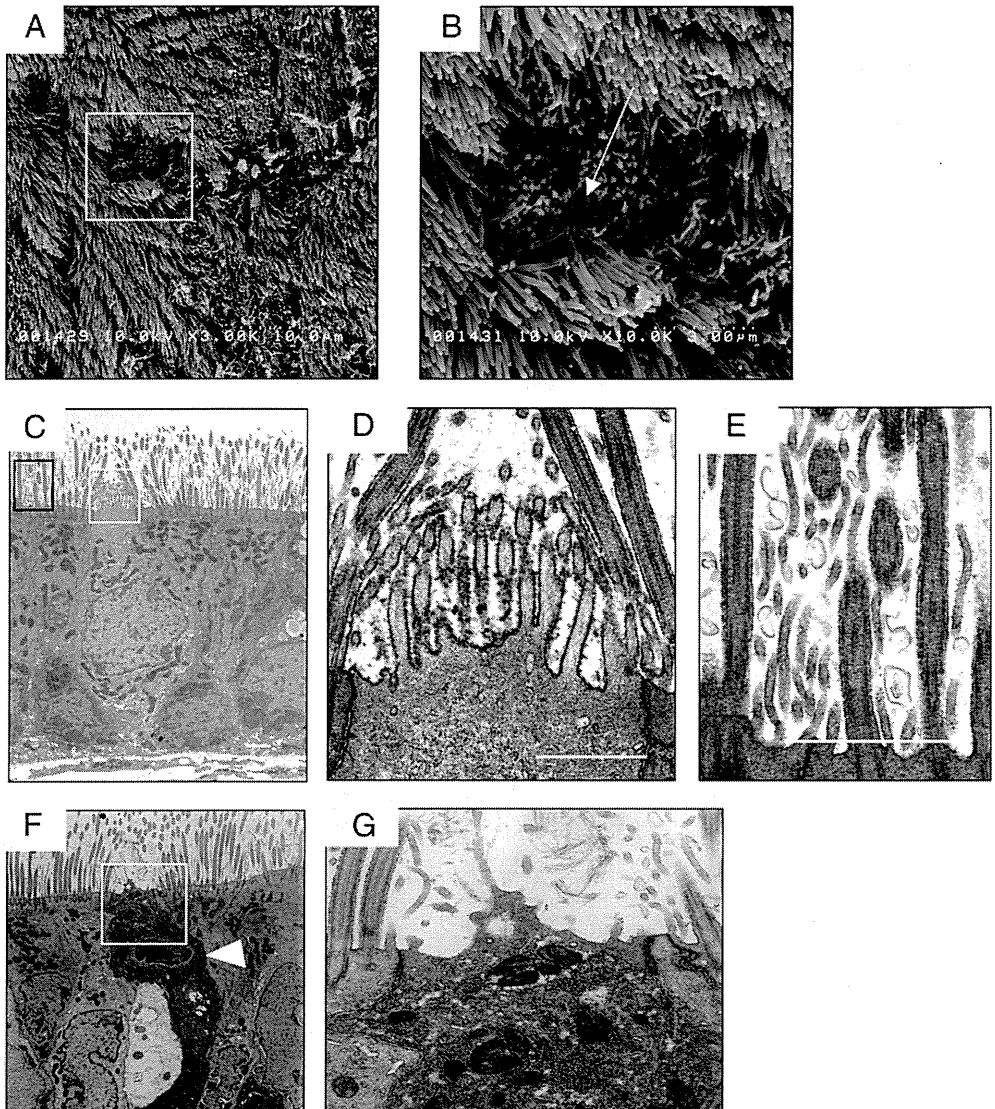

FIGURE 2. Electron microscopic analysis of respiratory M cells. *A* and *B*, SEM analysis shows that the M cells (*B*, arrow) in the nasal passage epithelium are distinguishable from adjacent respiratory epithelial cells by their relatively depressed and dark brush borders. An enlargement of the area in the rectangle in *A* is shown in *B*. As indicated in the *Materials and Methods*, the tissue specimen was incubated with HRP-conjugated UEA-1 before TEM analysis. *C–E*, TEM analysis of respiratory M cells reveals shorter and more irregular microvilli with definite UEA-1$^+$ signals (*D*), unlike the cilia of neighboring respiratory epithelial cells (*E*). *F* and *G*, TEM analysis of NALT M cells. A readily apparent intraepithelial pocket with mononuclear cells (*F*, arrowhead) and short microvilli on the apical surfaces of NALT M cells are seen. The white squares in *C* and *F* indicate UEA-1$^+$ respiratory and NALT M cells, respectively, and are magnified in *D* and *G*, respectively. The black rectangle in *C* indicates an adjacent respiratory epithelial cell and is magnified in *E*. *C–G*, Scale bars, 0.5 μm. Results are representative of four independent experiments.

Protein and bacterial Ag uptake by respiratory M cells

Because M cells were frequently found in the single layer of nasal passage epithelium (Fig. 1*D–G*), we next examined the ability of respiratory M cells to take up various forms of Ag from the lumen of the nasal cavity. DQ OVA or recombinant *Salmonella typhimurium* expressing GFP (*Salmonella*-GFP) was instilled into the nasal cavities of BALB/c mice via the nares. Thirty minutes after the intranasal instillation, immunohistological analyses revealed that the M cells located on the lateral surfaces of the nasal turbinates in the single layer of nasal epithelium had taken up DQ OVA (Fig. 3*A*, 3*B*), as had the M cells located in the NALT epithelium (Fig. 3*C*). Recombinant *Salmonella*-GFP was also observed in M cells in the single layer of nasal epithelium after intranasal administration (Fig. 4*A*, 4*B*). These findings demonstrate that, like NALT M cells (Figs. 3*C*, 4*C*), respiratory M cells were capable of taking up both soluble protein and bacterial Ags.

To further demonstrate the biological significance of respiratory M cells, the numbers of these M cells per mouse were examined and compared with those of NALT M cells (Fig. 3*D*). The number of respiratory M cells was significantly higher than that of NALT M cells. Next, we examined the efficiency of Ag uptake per respiratory M cell and NALT M cell (Figs. 3*E–J*, 4*D–I*). Nasal passage and NALT epithelial cells isolated from BALB/c mice 30 min after intranasal instillation of DQ OVA or recombinant *Salmonella*-GFP were counterstained with PE–UEA-1 for flow cytometric analysis. The UEA-1$^+$ fraction showed a significantly greater efficiency of uptake of DQ OVA Ag and recombinant *Salmonella*-GFP than did UEA-1$^-$ cells isolated from the re-

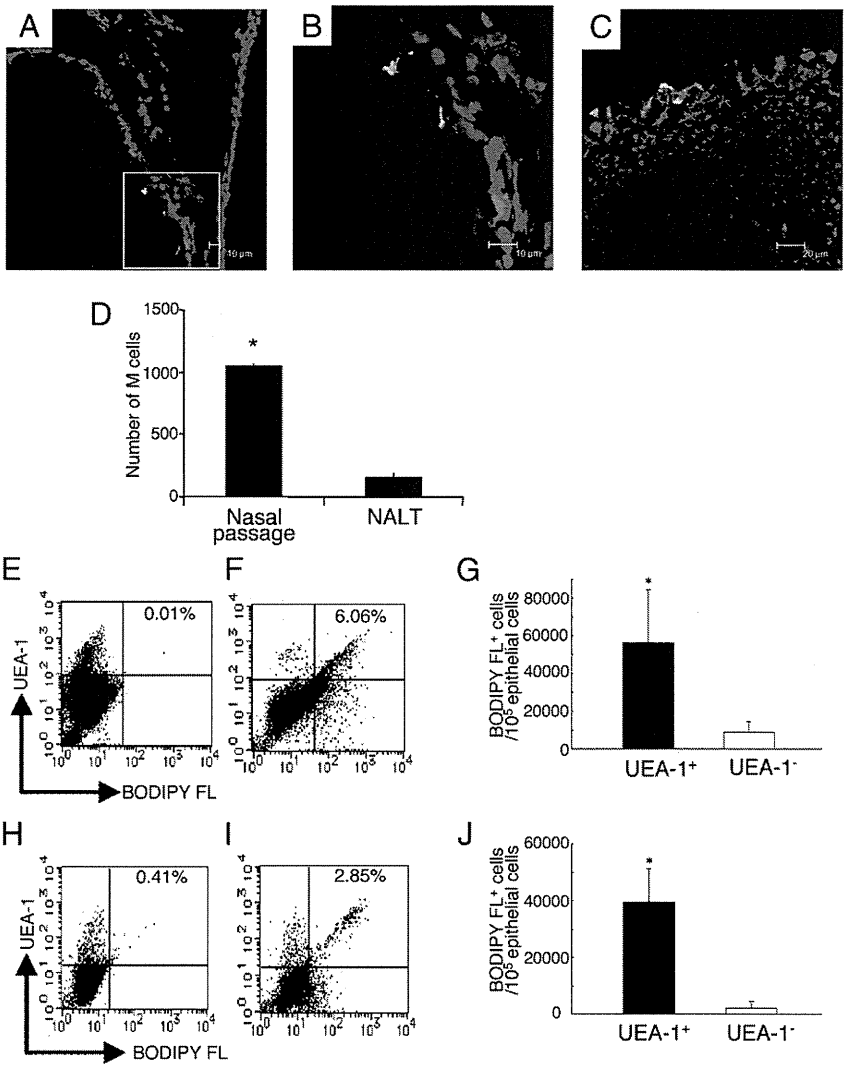

FIGURE 3. Respiratory M cells can take up DQ OVA. *A* and *B*, Immunofluorescence staining of nasal passages in BALB/c mice 30 min after DQ OVA (0.5 mg, green) instillation. Frozen sections of nasal passage were stained with rhodamine–UEA-1 (red) and DAPI (blue). Scale bars, 10 μm. The merged image is shown in *A*. An enlargement of the area in the rectangle in *A* is shown in *B*. These pictures demonstrate DQ OVA uptake by UEA-1$^+$ respiratory M cells. *C*, UEA-1$^+$ (red) NALT M cells in BALB/c mice also show an ability to take up DQ OVA (green). Scale bar, 20 μm. The results are representative of seven independent experiments. *D*, The numbers of UEA-1$^+$WGA$^-$ cells in nasal passages and NALT were quantified. The results are representative of four independent experiments. Flow cytometric analysis of DQ OVA uptake by UEA-1$^+$ respiratory (*E–G*) and NALT (*H–J*) M cells 30 min after intranasal instillation of PBS (*E*, *H*; control) or DQ OVA (*F*, *I*). *G* and *J*, UEA-1$^+$ cells showed significantly higher uptake of DQ OVA than did UEA-1$^-$ cells in the nasal passages and NALT. The results are representative of four independent experiments. *$p < 0.05$.

spiratory epithelium of the nasal passage (Figs. 3*E–G*, 4*D–F*) and NALT (Figs. 3*H–J*, 4*G–I*).

Three-dimensional confocal microscopic analysis demonstrated that UEA-1$^+$ GFP$^+$ cells, which were sorted from the nasal passages of the mice intranasally infected with GFP-*Salmonella*, had captured and taken up the bacteria (Fig. 4*J*, Supplemental Video 1).

Cluster formation by respiratory M cells and DCs in response to inhaled respiratory pathogens

Because respiratory M cells are capable of capturing bacterial Ag, we considered it important to assess these cells as potential new entry sites for respiratory pathogens such as GAS. Confocal microscopic analysis demonstrated that, after its intranasal instillation, GAS stained with FITC–anti-*Streptococcus* A Ab was taken up by UEA-1$^+$ respiratory M cells (Fig. 5*B–E*). SEM analysis also revealed the presence of GAS-like microorganisms on the membranes of respiratory M cells after nasal challenge with GAS (Supplemental Fig. 2*A*). As one might expect, GAS were found in UEA-1$^+$ NALT M cells (Supplemental Fig. 2*B*) as well, confirming a previously reported result (20). Our findings suggest that respiratory M cells act as alternative entry sites for respiratory pathogens.

When we examined the site of invasion by GAS, we noted the presence of CD11c$^+$ DCs underneath the respiratory M cells (Fig. 5). Confocal microscopic analysis of the nasal passage epithelium after intranasal instillation of GAS revealed evidence of the recruitment of DCs, some having contact with the GAS, to the area underneath the respiratory M cells (Fig. 5*B–E*). A few DCs were also observed in the nasal passages of naive mice (Fig. 5*A*); these nasal DCs might preferentially migrate to the area underneath the respiratory M cells to receive Ags from these cells for the initiation of Ag-specific immune responses.

Presence of respiratory M cells in NALT-deficient mice

When we examined the numbers of respiratory M cells in the lymphoid structure-deficient Id2$^{-/-}$ mice (including NALT, NALT-null), the frequency of occurrence of respiratory M cells was comparable to that found in their littermate Id2$^{+/-}$ mice (Fig. 6*A*). This finding suggested that development of respiratory M cells occurred normally under NALT-null or Id2-deficient conditions. Frozen tissue samples were next prepared from NALT-null mice that had received fluorescence-labeled bacteria by intranasal instillation. Immunohistological analysis of these samples revealed the presence of recombinant *Salmonella*-GFP in UEA-1$^+$ cells from the nasal epithelium of Id2$^{-/-}$ mice. GFP-positive bacteria were also located in the subepithelial region of the nasal passages, suggesting that, in the NALT-null mice, some of the nasally deposited bacteria were taken up by respiratory M cells (Fig. 6*B*, 6*C*). Flow cytometric analysis confirmed the uptake of recombinant *Salmonella*-GFP by UEA-1$^+$ M cells, with UEA-1$^+$ cells in the nasal passages of Id2$^{-/-}$ mice showing a significantly higher uptake than UEA-1$^-$ cells (Fig. 6*D–F*).

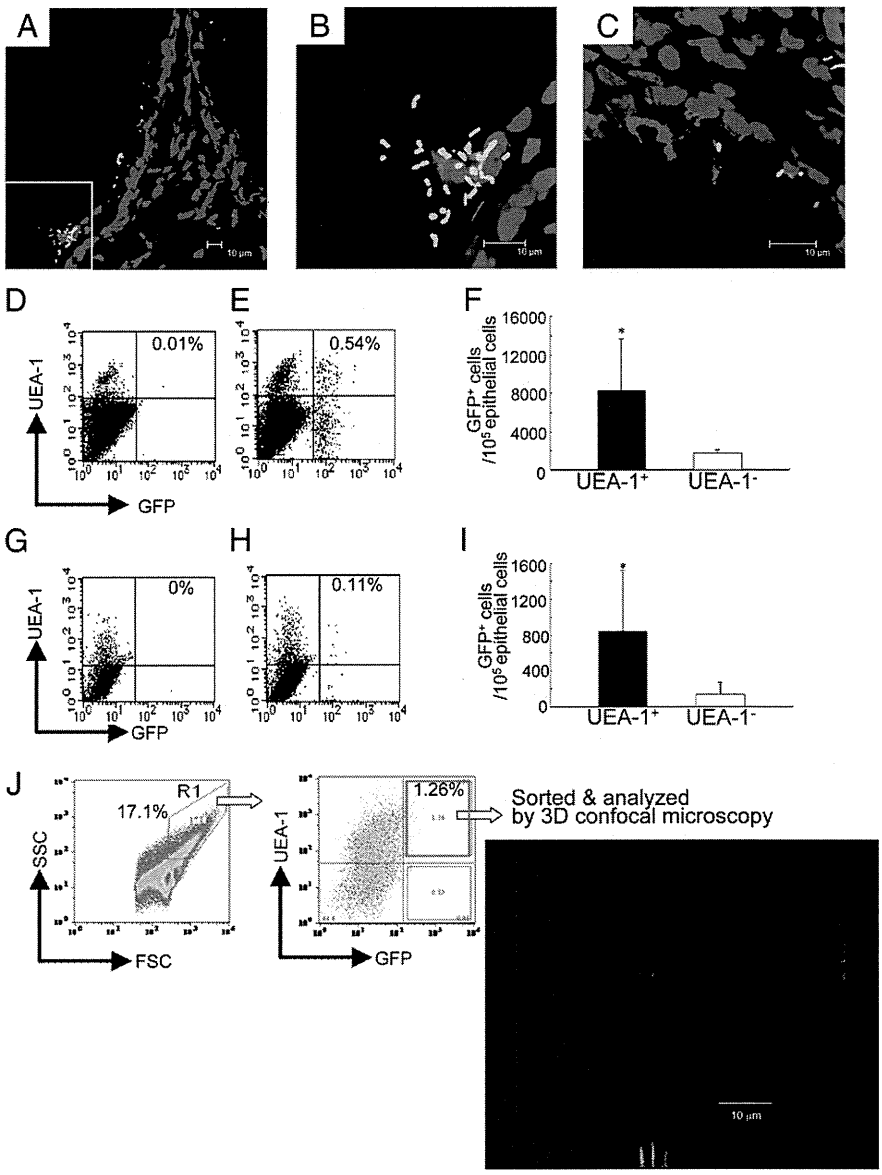

FIGURE 4. Respiratory M cells show an ability to take up recombinant *Salmonella*-GFP. *A* and *B*, Immunofluorescence staining of the nasal passages of BALB/c mice 30 min after GFP-*Salmonella* (5×10^8 CFU, green) instillation. Frozen sections of nasal passage were stained with rhodamine–UEA-1 (red) and DAPI (blue). The merged image is shown in *A*. An enlargement of the area in the rectangle in *A* is shown in *B*. These pictures demonstrate the ability of UEA-1^+ respiratory M cells, like UEA-1^+ NALT M cells (*C*), to take up GFP-*Salmonella*. The results are representative of six separate experiments. *A–C*, Scale bars, 10 μm. Flow cytometric analysis of GFP-*Salmonella* uptake by UEA-1^+ respiratory (*D–F*) and NALT (*G–I*) M cells 30 min after intranasal instillation of PBS (*D*, *G*; control) or GFP-*Salmonella* (*E*, *H*). *F* and *I*, Efficiency of uptake of GFP-*Salmonella* by UEA-1^+ cells in both nasal passages and NALT. The data showed UEA-1^+ M cells to be significantly more efficient than UEA-1^- epithelial cells at taking up GFP-*Salmonella*. The results are representative of five independent experiments. *J*, Three-dimensional confocal microscopic analysis demonstrated that UEA-1^+ GFP^+ cells, which were sorted from the nasal passages of mice intranasally infected with GFP-*Salmonella* (green), took up bacteria. Scale bar, 10 μm. The results are representative of three separate experiments. $^*p < 0.05$.

Induction of Ag-specific immune responses in NALT-deficient mice

NALT-null ($Id2^{-/-}$) mice and their littermate $Id2^{+/-}$ mice were intranasally immunized with recombinant *S. typhimurium* BRD 847 expressing a 50-kDa ToxC fragment of tetanus toxin (recombinant *Salmonella*-ToxC) to examine whether Ag sampling via respiratory M cells could induce Ag-specific immune responses in NALT-deficient mice. To eliminate any possible GALT-associated induction of Ag-specific immune responses from the swallowing of bacterial solutions after intranasal immunization, mice were given drinking water containing gentamicin from 1 wk before the immunization to the end of the experiment and were also subjected to intragastric lavage with 500 μl gentamicin solution before and after intranasal immunization. This protocol successfully eliminated the possibility of the intranasally delivered bacteria becoming deposition in the intestine (Supplemental Fig. 1). The titer of TT-specific serum IgG Ab was as high in $Id2^{-/-}$ mice as in $Id2^{+/-}$ mice (Fig. 6*G*). TT-specific IgA Abs were also detected in the nasal secretions and vaginal washes of intranasally immunized NALT-deficient mice (Fig. 6*H*, 6*I*). As expected, TT-specific Abs were not detected in either $Id2^{-/-}$ or $Id2^{+/-}$ mice intranasally immunized with a control recombinant *Salmonella* that did not express the ToxC gene (Fig. 6*G–I*). In addition to the responses to *Salmonella*, GAS-specific immune responses were induced in the absence of NALT in the experiment with $Id2^{-/-}$ mice (Fig. 6*J–L*). These data indicate that the respiratory M cell is an important Ag-sampling site for the induction of Ag-specific local IgA and serum IgG immune responses.

Discussion

In this study, we show the existence of a novel Ag sampling site for inhaled Ags in the upper respiratory epithelium. The murine nasal membrane has been reported to contain four types of epithelium: respiratory, olfactory, transitional, and squamous (21). Most of the respiratory epithelium is located in the lateral and ventral regions of the nasal cavity and is covered with pseudostratified ciliated columnar cells (21). In this study, we were also able to observe a single-layer epithelium on the lateral surfaces of the turbinates, which was comprised exclusively of UEA-$1^+$$WGA^-$ M cells (Fig. 1). These respiratory M cells showed specific reactivity to our previously developed M cell-specific mAb NKM 16-2-4 (12). Because NALT is characterized by follicle-associated epithelium, we first thought that this single-layer epithelium could represent the follicle-associated epithelium of the nasal passage. However,

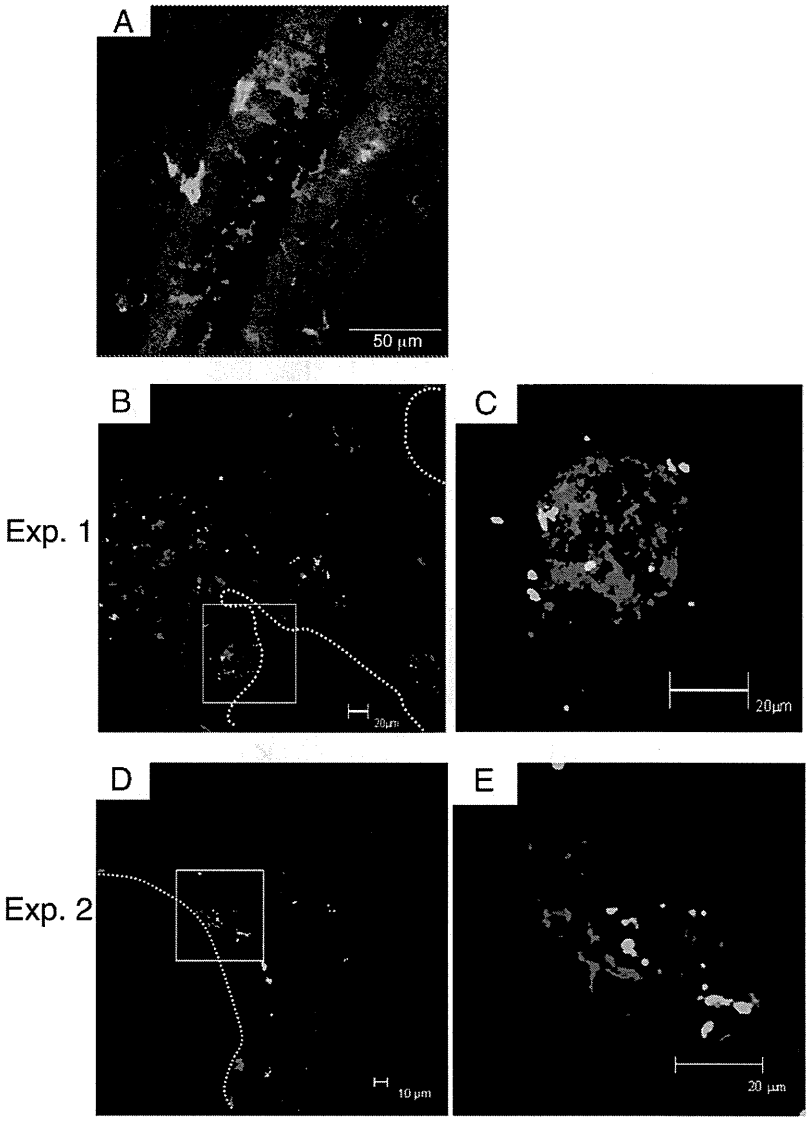

FIGURE 5. Respiratory M cells form clusters with DCs after GAS infection. *A*, Before nasal challenge with GAS, only a few DCs (FITC-CD11c$^+$, green) were associated with UEA-1$^+$ M cells (red) in the nasal passage. Scale bar, 50 μm. *B–E*, Two sets of confocal views of the nasal passage 5 d after intranasal instillation of GAS (Exp. 1 and Exp. 2, respectively). Frozen sections of the nasal passage were stained with FITC–anti-*Streptococcus* A Ab (green), rhodamine–UEA-1 (red), and allophycocyanin-CD11c (blue). These images reveal large numbers of DCs congregated underneath the UEA-1$^+$ respiratory M cells; some of the DCs were closely associated with GAS infiltrated through the UEA-1$^+$ respiratory M cells. *C* and *E* are enlargements of the areas in the squares shown in *B* and *D*, respectively. The results are representative of five independent experiments. *B*, *C*, and *E*, Scale bars, 20 μm; *D*, scale bar, 10 μm.

we ruled out this possibility when we could not find any organized lymphoid structures beneath the single-layer epithelium. The respiratory M cells had most of the classical features of M cells, including a depressed surface covered with short and irregular microvilli. However, TEM analysis revealed that, unlike NALT M cells, they lacked an intraepithelial pocket (Fig. 2). Examination of the numbers of respiratory and NALT M cells per nasal cavity revealed that there were more respiratory M cells than NALT M cells (in general six or seven times more; Fig. 3*D*), suggesting that the respiratory M cell plays a critical role as a gateway for the upper airway.

The anatomical and histological characteristics of the nasal cavity differ markedly between humans and mice. Reflecting this fact, the occurrence of single-layer epithelium also differs between the two species. Murine respiratory epithelium consists of a typical single-layer epithelium with traditional columnar epithelial cells in the turbinate portion of the nasal cavity, whereas pseudostratified columnar epithelium covers the olfactory epithelium (21, 22). In contrast, the traditional single-layer epithelium is not observed in the human nasal cavity, and both the upper respiratory surfaces and the olfactory surfaces are covered by pseudostratified columnar epithelium (23, 24). These differences suggest that the presence of respiratory M cells in the nasal cavity might be a feature unique to the mouse. The presence or absence of respiratory M cells in the human nasal cavity still needs to be carefully examined, and, if these cells are present, their contribution to the uptake of inhaled Ags needs to be investigated in future studies.

Previously, M cells in the lower respiratory tract were found to provide a portal of entry for bacterial pathogens into the lung (25). Our study suggests that the newly identified NALT-independent M cells in the upper respiratory tract provide an alternative portal of entry for nasally inhaled pathogens. The respiratory epithelium comprises three distinct Ag-sampling and/or pathogen-invasion sites: respiratory M cells and NALT M cells in the upper respiratory tract and M cells in the lower respiratory tract. It is interesting to speculate that the nature of the respiratory pathogen may dictate its preferred entry site, with GAS preferentially invading the host via the upper respiratory tract M cells and *Mycobacterium tuberculosis* preferentially invading via the lower respiratory tract M cells. This attractive possibility requires careful examination, and such a line of investigation has been initiated in our laboratory.

Salmonella, a known gastrointestinal pathogen, may have no relevance to the immunological and physiological aspects of Ag uptake by respiratory M cells. However, when used as a live vector for the intranasal delivery of vaccine Ags, attenuated *Salmonella* effectively elicits Ag-specific immune responses (26–29). Pasetti et al. (28) compared intranasal and orogastric immunizations in

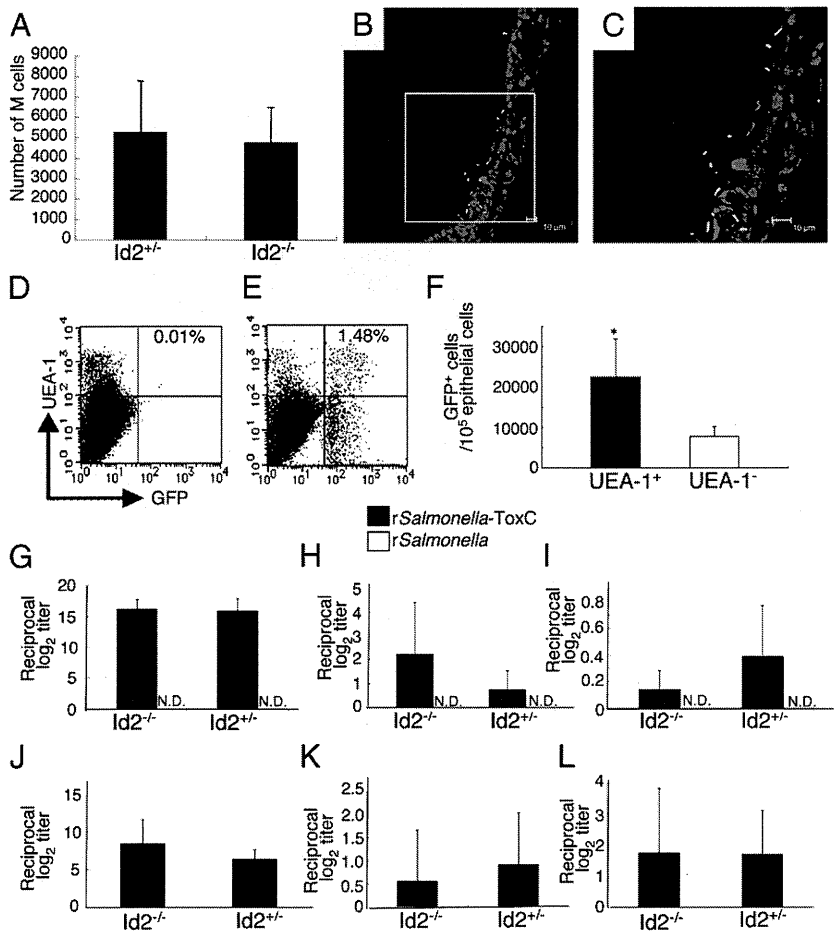

FIGURE 6. Id2$^{-/-}$ mice, which lack NALT, can take up GFP-*Salmonella*, which induce Ag-specific immune responses in UEA-1$^+$ respiratory M cells. *A*, The numbers of UEA-1$^+$WGA$^-$ cells in nasal passages of Id2$^{-/-}$ and Id2$^{+/-}$ mice were measured. The results are representative of four independent experiments. *B* and *C*, Immunofluorescence staining of nasal passages of Id2$^{-/-}$ mice in which GFP-expressing *Salmonella* (green) had been instilled. Frozen sections of nasal passages were stained with rhodamine–UEA-1 (red) and DAPI (blue). Scale bars, 10 μm. *C* is an enlargement of the area in the square shown in *B*. The results are representative of three independent experiments. *D–F*, Flow cytometric analysis of GFP-*Salmonella* uptake by UEA-1$^+$ M cells 30 min after intranasal instillation of PBS (*D*; control) or GFP-*Salmonella* (*E*) in the nasal passages of Id2$^{-/-}$ mice. *F*, Efficiency of uptake by UEA-1$^+$ cells in the nasal passages of Id2$^{-/-}$ mice was significantly greater than that by UEA-1$^-$ cells. The results are representative of three independent experiments. *G–I*, NALT-deficient (Id2$^{-/-}$) mice and Id2$^{+/-}$ mice were intranasally immunized with recombinant *Salmonella*-ToxC (2.5×10^8 CFU) or recombinant *Salmonella* (2.5×10^8) alone three times at weekly intervals. They were given gentamicin-containing drinking water and also subjected to intragastric lavage with gentamicin solution to eliminate GALT-mediated Ag-specific immune responses. Samples were obtained 7 d after the last intranasal immunization to measure TT-specific Igs by ELISA. Serum IgG (*G*), nasal wash IgA (*H*), vaginal wash IgA (*I*). The results are representative of three independent experiments. *J–L*, As was the case with *Salmonella*, GAS-specific immune responses were induced in the absence of NALT (i.e., in Id2$^{-/-}$ mice), this time by a single intranasal injection of GAS (2×10^8 CFU). Serum IgG (*J*), nasal wash IgA (*K*), vaginal wash IgA (*L*). There were no statistical differences between Id2$^{-/-}$ and Id2$^{+/-}$ mice, as analyzed by the unpaired Mann–Whitney *U* test. The results are representative of five independent experiments. *$p < 0.05$. N.D., not detected.

terms of both Ag-specific immune responses and in vivo distribution of vaccine organisms; they demonstrated that intranasal immunization resulted in greater humoral and cell-mediated immune responses and in the delivery of larger numbers of vaccine organisms to the nasal tissues, lungs, and Peyer's patches. Furthermore, intranasal immunization effectively induces Ag-specific IgA Abs in the reproductive secretions of mice and primates (30, 31). Notably, the levels of Ag-specific IgA Abs in the nasal secretions of NALT-deficient Id2$^{-/-}$ mice were not significantly higher than, or comparable to, those of control tissue-intact mice following intranasal immunization with recombinant *Salmonella* expressing ToxC (Fig. 6*H*) or GAS (Fig. 6*K*), respectively. In contrast, in intranasally immunized NALT-deficient mice, the levels of Ag-specific IgA Abs in remote secretions such as the vaginal wash were not significantly lower than, or comparable to, those in similarly treated tissue-intact mice (Fig. 6*I*, 6*L*). Inasmuch as these results revealed no significant differences between the two groups of intranasally immunized mice, our results at least suggest that respiratory M cells contribute to the induction of Ag-specific immune responses at both local and distant effector sites. However, we still need to carefully examine and compare the contributions of respiratory M cells and NALT M cells in the initiation of Ag-specific IgA Ab responses at local (e.g., airway) and distant (e.g., reproductive tract) effector sites.

In regard to the functional aspects of respiratory M cells, our data demonstrated that the numbers of respiratory M cells that took up OVA were comparable to those of NALT M cells (Fig. 3*G*, 3*J*). In contrast, 10 times more respiratory M cells than NALT M cells took up *Salmonella*; this result suggested that respiratory M cells are more efficient at taking up bacterial (or particulate) Ags than are NALT M cells (Fig. 4*F*, 4*I*). Although we do not have any data regarding the mechanism(s) behind these findings, these results

suggest that there may be functional differences in, for example, Ag uptake capability, between respiratory M cells and NALT M cells due to possible differences in the expression of bacterial Ag receptors, even though the morphologies and phenotypes of these two subsets of M cells are similar. In support of this possibility, it has been shown that the expression of a GP-2–specific receptor for FimH bacteria is restricted to Peyer's patches and not villous M cells; this situation may be analogous to that of NALT and respiratory M cells (32). Although the molecular mechanisms for the induction of Ag-specific immune responses by intranasal immunization and the efficacy of intranasal inoculation await elucidation, we demonstrated in this paper that respiratory M cells, like NALT M cells, are capable of sampling *Salmonella*, thereby opening a new avenue for the uptake of *Salmonella*-delivered vaccine.

CD18-expressing phagocytes (33) and mucosal DCs (34) are involved in the uptake of pathogens from the lumen of the intestine, but their role in the upper respiratory tract has never been clarified. Moreover, we found no evidence that mucosal DCs take up pathogens from the lumen of the nasal passage by expanding their dendrites into the lumen after nasal challenge with GAS. It was recently shown that intranasal immunization of mice with OVA plus adenovirus vector expressing Flt3 ligand as a mucosal adjuvant selectively increases $CD11b^+$ DC numbers in the nasal passages more effectively than those in NALT and subsequently induces Ag-specific Ab and CTL responses (35). Therefore, we speculated that the induction of immune responses in the murine model of intranasal administration of bacteria (e.g., *Salmonella* and GAS) might depend on the presence of appropriate initial Ag sampling sites associated with M cells, which can internalize the vaccine organisms. In this study, DCs were rarely detected in the subepithelial layer or the epithelial layer of the nasal passage in naive mice (Fig. 5*A*). It is important to note that DCs migrated to the area underneath the respiratory M cells and accumulated there to form cell clusters after exposure to respiratory pathogens (Fig. 5*B–D*). Following mucosal exposure to pathogens, submucosal DCs accumulate underneath infected mucosal epithelium that is not associated with organized lymphoid follicles (36, 37). Furthermore, these Ag-capturing DCs are capable of migrating into the draining lymph nodes (dLNs), where they encounter naive T cells for initial Ag-priming (36, 37). The question of whether DCs resident in the nasal passages migrate to the submucosal area to receive inhaled pathogens taken up via respiratory M cells and then travel to the dLNs (e.g., the cervical lymph nodes) to initiate an Ag-specific immune response remains to be addressed. It is interesting to postulate that respiratory M cells could be alternative airway Ag sampling sites for subsequent processing or presentation by nasal passage DCs, thereby initiating Ag-specific immune responses in the dLNs. In support of this hypothesis, it has been shown that Ag-specific Th cells are generated and found in the NALT and dLNs of mice given GAS intranasally (38). Our current study offers proof in support of this hypothesis by showing that *Salmonella* were effectively taken up by upper respiratory tract M cells in NALT and respiratory M cells and that a live vector-containing vaccine Ag induced Ag-specific immune responses via the nasal route.

We showed that TT-specific serum IgG and nasal wash IgA immune responses after intranasal immunization with recombinant *Salmonella*-ToxC were as high in $Id2^{-/-}$ mice as in $Id2^{+/-}$ mice (Fig. 6*G*, 6*H*) and that the frequency of occurrence of respiratory M cells in $Id2^{-/-}$ mice was comparable to that in their littermate $Id2^{+/-}$ mice (Fig. 6*A*). Generally, as discussed above, submucosal and dermal DCs have been shown to migrate to (or to be located in) the area just beneath infected epithelium and to then migrate into the dLNs after they have captured Ags. The DCs then present the peptides derived from these Ags to naive T cells, which subsequently undergo differentiation to Ag-specific effector T cells (36, 37). It has further been suggested that, rather than the DCs harboring Ag-derived peptides migrating to the systemic compartments, such as spleen and other secondary lymphoid tissues, the effector T cells generated in the dLNs after mucosal or vaginal Ag application migrate to these compartments and initiate Ag-specific immune responses (36).

If the cross-talk system between the airway mucosal and systemic immune compartments is similar to that between the reproductive mucosal and systemic immune compartments, it is unlikely that, in $Id2^{-/-}$ mice, the initiation of Ag-specific immune responses, including the presentation of Ags to naive T cells, occurs through migration of nasal DCs into the spleen after the capture of GAS-Ags by respiratory M cells and DCs. However, we cannot rule out this possibility, because it is possible that the nasal immune system, including the system by which Ags are taken up by respiratory M cells, offers distinct Ag-capture, -processing, and -presentation mechanisms via nasal DCs for the generation and migration of Ag-specific effector T cell and B cells. We have also found B-1 cell populations in the nasal passages (N. Tanaka, S. Fukuyama, T. Nagatake, K. Okada, M. Murata, K. Goda, D-Y. Kim, T. Nochi, S. Sato, J. Kunisawa, T. Kaisho, Y. Kurono, and H. Kiyono, manuscript in preparation), and it is possible that these cells may contribute to the induction of Ag-specific Ig responses without any help from $CD4^+$ T cells. At this stage, this is mere speculation, and the precise mechanism needs to be addressed in the future.

Taken together, these findings led us to conclude that respiratory M cells are effective alternative sampling sites for nasally inhaled bacterial Ags and thus play a key role in the induction of systemic and local mucosal immune responses.

Acknowledgments

We thank the staff of the Division of Mucosal Immunology, Institute of Medical Science and the University of Tokyo for technical advice and helpful discussions.

Disclosures

The authors have no financial conflicts of interest.

References

1. Kiyono, H., and S. Fukuyama. 2004. NALT- versus Peyer's-patch-mediated mucosal immunity. *Nat. Rev. Immunol.* 4: 699–710.
2. Yuki, Y., and H. Kiyono. 2003. New generation of mucosal adjuvants for the induction of protective immunity. *Rev. Med. Virol.* 13: 293–310.
3. Fukuyama, S., T. Hiroi, Y. Yokota, P. D. Rennert, M. Yanagita, N. Kinoshita, S. Terawaki, T. Shikina, M. Yamamoto, Y. Kurono, and H. Kiyono. 2002. Initiation of NALT organogenesis is independent of the IL-7R, LTbetaR, and NIK signaling pathways but requires the Id2 gene and CD3(-)CD4(+)CD45(+) cells. *Immunity* 17: 31–40.
4. Hiroi, T., K. Iwatani, H. Iijima, S. Kodama, M. Yanagita, and H. Kiyono. 1998. Nasal immune system: distinctive Th0 and Th1/Th2 type environments in murine nasal-associated lymphoid tissues and nasal passage, respectively. *Eur. J. Immunol.* 28: 3346–3353.
5. Shikina, T., T. Hiroi, K. Iwatani, M. H. Jang, S. Fukuyama, M. Tamura, T. Kubo, H. Ishikawa, and H. Kiyono. 2004. IgA class switch occurs in the organized nasopharynx- and gut-associated lymphoid tissue, but not in the diffuse lamina propria of airways and gut. *J. Immunol.* 172: 6259–6264.
6. Shimoda, M., T. Nakamura, Y. Takahashi, H. Asanuma, S. Tamura, T. Kurata, T. Mizuochi, N. Azuma, C. Kanno, and T. Takemori. 2001. Isotype-specific selection of high affinity memory B cells in nasal-associated lymphoid tissue. *J. Exp. Med.* 194: 1597–1607.
7. Debertin, A. S., T. Tschernig, H. Tönjes, W. J. Kleemann, H. D. Tröger, and R. Pabst. 2003. Nasal-associated lymphoid tissue (NALT): frequency and localization in young children. *Clin. Exp. Immunol.* 134: 503–507.
8. Wiley, J. A., M. P. Tighe, and A. G. Harmsen. 2005. Upper respiratory tract resistance to influenza infection is not prevented by the absence of either nasal-associated lymphoid tissue or cervical lymph nodes. *J. Immunol.* 175: 3186–3196.

9. Lund, F. E., S. Partida-Sánchez, B. O. Lee, K. L. Kusser, L. Hartson, R. J. Hogan, D. L. Woodland, and T. D. Randall. 2002. Lymphotoxin-alpha-deficient mice make delayed, but effective, T and B cell responses to influenza. *J. Immunol.* 169: 5236–5243.
10. Rangel-Moreno, J., J. Moyron-Quiroz, K. Kusser, L. Hartson, H. Nakano, and T. D. Randall. 2005. Role of CXC chemokine ligand 13, CC chemokine ligand (CCL) 19, and CCL21 in the organization and function of nasal-associated lymphoid tissue. *J. Immunol.* 175: 4904–4913.
11. Yokota, Y., A. Mansouri, S. Mori, S. Sugawara, S. Adachi, S. Nishikawa, and P. Gruss. 1999. Development of peripheral lymphoid organs and natural killer cells depends on the helix-loop-helix inhibitor Id2. *Nature* 397: 702–706.
12. Nochi, T., Y. Yuki, A. Matsumura, M. Mejima, K. Terahara, D. Y. Kim, S. Fukuyama, K. Iwatsuki-Horimoto, Y. Kawaoka, T. Kohda, et al. 2007. A novel M cell-specific carbohydrate-targeted mucosal vaccine effectively induces antigen-specific immune responses. *J. Exp. Med.* 204: 2789–2796.
13. Jang, M. H., M. N. Kweon, K. Iwatani, M. Yamamoto, K. Terahara, C. Sasakawa, T. Suzuki, T. Nochi, Y. Yokota, P. D. Rennert, et al. 2004. Intestinal villous M cells: an antigen entry site in the mucosal epithelium. *Proc. Natl. Acad. Sci. USA* 101: 6110–6115.
14. Hopkins, S. A., F. Niedergang, I. E. Corthesy-Theulaz, and J. P. Kraehenbuhl. 2000. A recombinant *Salmonella typhimurium* vaccine strain is taken up and survives within murine Peyer's patch dendritic cells. *Cell. Microbiol.* 2: 59–68.
15. Niedergang, F., J. C. Sirard, C. T. Blanc, and J. P. Kraehenbuhl. 2000. Entry and survival of *Salmonella typhimurium* in dendritic cells and presentation of recombinant antigens do not require macrophage-specific virulence factors. *Proc. Natl. Acad. Sci. USA* 97: 14650–14655.
16. Chatfield, S. N., I. G. Charles, A. J. Makoff, M. D. Oxer, G. Dougan, D. Pickard, D. Slater, and N. F. Fairweather. 1992. Use of the nirB promoter to direct the stable expression of heterologous antigens in *Salmonella* oral vaccine strains: development of a single-dose oral tetanus vaccine. *Biotechnology (N. Y.)* 10: 888–892.
17. Yamamoto, M., P. Rennert, J. R. McGhee, M. N. Kweon, S. Yamamoto, T. Dohi, S. Otake, H. Bluethmann, K. Fujihashi, and H. Kiyono. 2000. Alternate mucosal immune system: organized Peyer's patches are not required for IgA responses in the gastrointestinal tract. *J. Immunol.* 164: 5184–5191.
18. Todome, Y., H. Ohkuni, K. Yokomuro, Y. Kimura, S. Hamada, K. H. Johnston, and J. B. Zabriskie. 1988. Enzyme-linked immunosorbent assay of antibody to group A *Streptococcus*-specific C carbohydrate with trypsin-pronase-treated whole cells as antigen. *J. Clin. Microbiol.* 26: 464–470.
19. Matulionis, D. H., and H. F. Parks. 1973. Ultrastructural morphology of the normal nasal respiratory epithelium of the mouse. *Anat. Rec.* 176: 64–83.
20. Park, H. S., K. P. Francis, J. Yu, and P. P. Cleary. 2003. Membranous cells in nasal-associated lymphoid tissue: a portal of entry for the respiratory mucosal pathogen group A *streptococcus. J. Immunol.* 171: 2532–2537.
21. Mery, S., E. A. Gross, D. R. Joyner, M. Godo, and K. T. Morgan. 1994. Nasal diagrams: a tool for recording the distribution of nasal lesions in rats and mice. *Toxicol. Pathol.* 22: 353–372.
22. Adams, D. R. 1972. Olfactory and non-olfactory epithelia in the nasal cavity of the mouse, Peromyscus. *Am. J. Anat.* 133: 37–49.
23. Cagici, C. A., G. Karabay, C. Yilmazer, S. Gencay, and O. Cakmak. 2005. Electron microscopy findings in the nasal mucosa of a patient with stenosis of the nasal vestibule. *Int. J. Pediatr. Otorhinolaryngol.* 69: 399–405.
24. Jafek, B. W., B. Murrow, R. Michaels, D. Restrepo, and M. Linschoten. 2002. Biopsies of human olfactory epithelium. *Chem. Senses* 27: 623–628.
25. Teitelbaum, R., W. Schubert, L. Gunther, Y. Kress, F. Macaluso, J. W. Pollard, D. N. McMurray, and B. R. Bloom. 1999. The M cell as a portal of entry to the lung for the bacterial pathogen *Mycobacterium tuberculosis. Immunity* 10: 641–650.
26. Galen, J. E., O. G. Gomez-Duarte, G. A. Losonsky, J. L. Halpern, C. S. Lauderbaugh, S. Kaintuck, M. K. Reymann, and M. M. Levine. 1997. A murine model of intranasal immunization to assess the immunogenicity of attenuated *Salmonella typhi* live vector vaccines in stimulating serum antibody responses to expressed foreign antigens. *Vaccine* 15: 700–708.
27. Locht, C. 2000. Live bacterial vectors for intranasal delivery of protective antigens. *Pharm. Sci. Technol. Today* 3: 121–128.
28. Pasetti, M. F., T. E. Pickett, M. M. Levine, and M. B. Sztein. 2000. A comparison of immunogenicity and in vivo distribution of *Salmonella enterica* serovar *Typhi* and *Typhimurium* live vector vaccines delivered by mucosal routes in the murine model. *Vaccine* 18: 3208–3213.
29. Pasetti, M. F., R. Salerno-Gonçalves, and M. B. Sztein. 2002. *Salmonella enterica* serovar *Typhi* live vector vaccines delivered intranasally elicit regional and systemic specific CD8+ major histocompatibility class I-restricted cytotoxic T lymphocytes. *Infect. Immun.* 70: 4009–4018.
30. Sakaue, G., T. Hiroi, Y. Nakagawa, K. Someya, K. Iwatani, Y. Sawa, H. Takahashi, M. Honda, J. Kunisawa, and H. Kiyono. 2003. HIV mucosal vaccine: nasal immunization with gp160-encapsulated hemagglutinating virus of Japan-liposome induces antigen-specific CTLs and neutralizing antibody responses. *J. Immunol.* 170: 495–502.
31. Imaoka, K., C. J. Miller, M. Kubota, M. B. McChesney, B. Lohman, M. Yamamoto, K. Fujihashi, K. Someya, M. Honda, J. R. McGhee, and H. Kiyono. 1998. Nasal immunization of nonhuman primates with simian immunodeficiency virus p55gag and cholera toxin adjuvant induces Th1/Th2 help for virus-specific immune responses in reproductive tissues. *J. Immunol.* 161: 5952–5958.
32. Hase, K., K. Kawano, T. Nochi, G. S. Pontes, S. Fukuda, M. Ebisawa, K. Kadokura, T. Tobe, Y. Fujimura, S. Kawano, et al. 2009. Uptake through glycoprotein 2 of FimH(+) bacteria by M cells initiates mucosal immune response. *Nature* 462: 226–230.
33. Vazquez-Torres, A., J. Jones-Carson, A. J. Bäumler, S. Falkow, R. Valdivia, W. Brown, M. Le, R. Berggren, W. T. Parks, and F. C. Fang. 1999. Extraintestinal dissemination of *Salmonella* by CD18-expressing phagocytes. *Nature* 401: 804–808.
34. Rescigno, M., M. Urbano, B. Valzasina, M. Francolini, G. Rotta, R. Bonasio, F. Granucci, J. P. Kraehenbuhl, and P. Ricciardi-Castagnoli. 2001. Dendritic cells express tight junction proteins and penetrate gut epithelial monolayers to sample bacteria. *Nat. Immunol.* 2: 361–367.
35. Sekine, S., K. Kataoka, Y. Fukuyama, Y. Adachi, J. Davydova, M. Yamamoto, R. Kobayashi, K. Fujihashi, H. Suzuki, D. T. Curiel, et al. 2008. A novel adenovirus expressing Flt3 ligand enhances mucosal immunity by inducing mature nasopharyngeal-associated lymphoreticular tissue dendritic cell migration. *J. Immunol.* 180: 8126–8134.
36. Zhao, X., E. Deak, K. Soderberg, M. Linehan, D. Spezzano, J. Zhu, D. M. Knipe, and A. Iwasaki. 2003. Vaginal submucosal dendritic cells, but not Langerhans cells, induce protective Th1 responses to herpes simplex virus-2. *J. Exp. Med.* 197: 153–162.
37. Allan, R. S., C. M. Smith, G. T. Belz, A. L. van Lint, L. M. Wakim, W. R. Heath, and F. R. Carbone. 2003. Epidermal viral immunity induced by CD8α^+ dendritic cells but not by Langerhans cells. *Science* 301: 1925–1928.
38. Park, H. S., M. Costalonga, R. L. Reinhardt, P. E. Dombek, M. K. Jenkins, and P. P. Cleary. 2004. Primary induction of CD4 T cell responses in nasal associated lymphoid tissue during group A streptococcal infection. *Eur. J. Immunol.* 34: 2843–2853.

Advanced Drug Delivery Reviews 64 (2012) 523–530

Contents lists available at ScienceDirect

Advanced Drug Delivery Reviews

journal homepage: www.elsevier.com/locate/addr

Gut-associated lymphoid tissues for the development of oral vaccines ☆

Jun Kunisawa [a,b,d,*], Yosuke Kurashima [a,c], Hiroshi Kiyono [a,b,c,d]

[a] Division of Mucosal Immunology, Department of Microbiology and Immunology, Institute of Medical Science, The University of Tokyo, Tokyo, Japan
[b] Department of Medical Genome Science, Graduate School of Frontier Science, The University of Tokyo, Tokyo, Japan
[c] Graduate School of Medicine, The University of Tokyo, Tokyo, Japan
[d] Core Research for Evolutional Science and Technology (CREST), Japan Science and Technology Agency, Tokyo, Japan

ARTICLE INFO

Article history:
Received 24 May 2011
Accepted 10 July 2011
Available online 30 July 2011

Keywords:
Mucosal vaccine
Peyer's patch
GALT
M cells

ABSTRACT

Oral vaccine has been considered to be a prospective vaccine against many pathogens especially invading across gastrointestinal tracts. One key element of oral vaccine is targeting efficient delivery of antigen to gut-associated lymphoid tissue (GALT), the inductive site in the intestine where antigen-specific immune responses are initiated. Various chemical and biological antigen delivery systems have been developed and some are in clinical trials. In this review, we describe the immunological features of GALT and the current status of antigen delivery system candidates for successful oral vaccine.

Contents

1. Introduction

Despite physical and biological barriers, the gastrointestinal tract is a major route of entry for numerous pathogens. Barriers include epithelial cells (EC) joined firmly by tight junction proteins, brush-border microvilli, and a dense layer of mucin [1]. Antimicrobial peptides, such as defensins produced by ECs and Paneth cells, are additional barrier to provide further protection [2].

☆ This review is part of the *Advanced Drug Delivery Reviews* theme issue on "Advances in Oral Drug Delivery: Improved Bioavailability of Poorly Absorbed Drugs by Tissue and Cellular Optimization".

* Corresponding author at: Division of Mucosal Immunology, Department of Microbiology and Immunology, Institute of Medical Science, The University of Tokyo 4-6-1 Shirokanedai, Minato-ku, Tokyo 108-8639, Japan. Tel.: +81 3 5449 5274; fax: +81 3 5449 5411.
E-mail address: kunisawa@ims.u-tokyo.ac.jp (J. Kunisawa).

0169-409X/$ – see front matter © 2011 Elsevier B.V. All rights reserved.
doi:10.1016/j.addr.2011.07.003

In addition to these barriers, the gastrointestinal tract includes immunological defense system, in particular secretory-immunoglobulin A (IgA) [3], which is predominantly produced at intestinal mucosa by the harmonious interaction between ECs and mucosal lymphocytes and blocks microbial infections by inhibiting adherence of mucosal pathogens at the intestinal lumen to host ECs. Secretory IgA (SIgA) can also neutralize toxins produced by gut pathogens by binding to biologically active sites of toxins.

The immunological characteristics of the gastrointestinal tract have focused attention on the development of effective oral vaccines. Oral vaccination offers several advantages over parenteral vaccination, including needle-free delivery, easy and comfortable administration, and the possibility of self-delivery. Most importantly, oral vaccination can induce both mucosal and systemic immunity, leading to the double layers of protective immune responses [4]. In contrast, parenteral immunization primarily yields a systemic immune response. Therefore, effective oral vaccination could establish a first line of immunological defense in the intestinal tract, a major site of pathogen entry, as well as promote immune surveillance perhaps at other mucosal and systemic sites. One of the major strategies of oral vaccine has been induction of pathogen- or toxin-specific SIgA.

The hostile environment of the gastrointestinal tract (low pH, presence of digestive enzymes, and the detergent activity of bile salts) often makes it difficult to induce protective immune responses by oral vaccination with antigen alone. Additionally, effective oral delivery of antigen to the induction site of the mucosal immune system (e.g., gut-associated lymphoid tissues :GALT) is made difficult by the significant dilution and dispersion of antigen that occurs in the lumen since a total interior area of the intestinal wall is thought to be equivalent to over one tennis coat surface. Further, physical barriers, such as mucus and the tight junctions between the ECs prevent the effective delivery of vaccine antigen. To overcome these obstacles, effort has focused on development of effective antigen delivery systems. In this review, we describe the immunological features of gut-associated lymphoid tissue as the most obvious target site of antigen delivery in the development of oral vaccines. We also describe the current strategies being used to develop versatile antigen delivery systems for efficient oral vaccination.

2. Immunological features of GALT

GALTs comprise several different organized lymphoid structures [5]. Among them, Peyer's patches (PPs) are well characterized as sites for the initiation of intestinal IgA responses. Isolated lymphoid tissue (ILF) is another GALT structure, which is also important in the induction of intestinal IgA responses.

2.1. Peyer's patches (PPs)

PPs are considered to be one of the largest organized lymphoid tissues in the gastrointestinal immune system. There are generally 8 to 10 PPs in the small intestine of mice and hundreds in humans [6]. Each PP is composed of several B cell-rich follicles surrounded by a mesh-like structure consisting of T cells known as interfollicular region (IFR) (Fig. 1).

Although PPs share some common immunological and micro-architectural features with peripheral secondary lymphoid organs, they are harboring unique features as the mucosa-associated lymphoid tissue [6]. For example, PPs contain efferent but not afferent lymphatics. To compensate, PPs are covered with a specialized epithelial region, termed follicle-associated epithelium (FAE), containing specialized antigen-sampling microfold or membranous cells (M cells). The M cells are characterized by short microvilli, a thin mucus layer, small cytoplasmic vesicles, and efficient transcytosis activity, allowing the selective and efficient transfer of antigens from the intestinal lumen into PPs (Fig. 2) [7]. Thus, M cells are considered

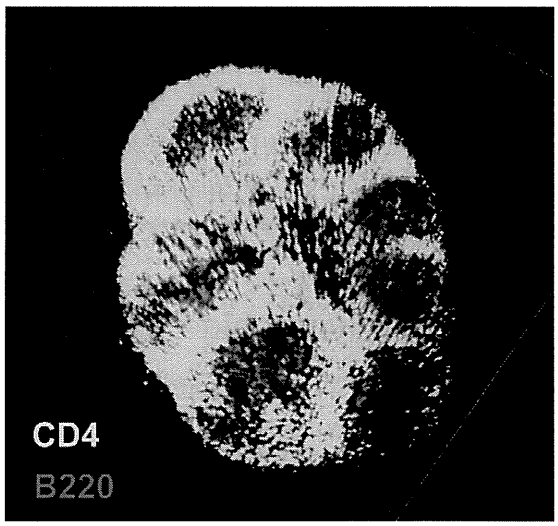

Fig. 1. Microarchitecture of murine Peyer's patches. Purified T cells (green) and B cells (red) were chemically labeled with carboxyfluorescein succinimidyl ester and arboxy SNARF-1, respectively, and adoptively transferred into mice. Fifteen hours after the transfer, cell distribution in the Peyer's patches was observed at the whole tissue level by using macro-confocal microscopy.

to be a professional antigen sampling and gateway cells for the mucosal immune system.

Dendritic cells (DCs) are abundant in the subepithelial dome region (SED) under the FAE, which thus can immediately take up orally encountered antigens from M cells and process and present antigenic peptides to mucosal T and B cells for the initiation of antigen-specific immune responses (Fig. 3). DCs are also found in the IFR. They are composed of at least three distinct subsets: $CD11c^+$ DCs in the SED, $CD8\alpha^+$ DCs in the T cell-rich IFRs, and double-negative DCs in both the SED and IFRs [8]. In addition to antigen presentation, DCs in the intestinal tissues express retinal dehydrogenase, an enzyme that converts vitamin A into retinoic acid. Retinoic acid promotes the preferential homing of activated antigen-specific T and B cells into the intestinal lamina propria by inducing the expression of gut imprinting molecules, such as $\alpha4\beta7$ integrin and CCR9 [9,10].

B cells, a major component of PP cells (~75%), are preferentially located in the follicle region (Figs. 1 and 3). Unlike other lymphoid organs, formation of germinal centers (GC) occurs in the PPs even under homeostatic conditions by the continuous stimulation from commensal bacteria, in which leads to the creation of molecular and

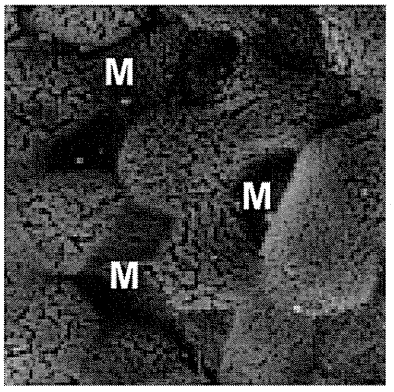

Fig. 2. Scanning electron micrograph of M cells in the Peyer's patches. Scanning electronic microscopy demonstrates that the M cells (indicated as "M") in the Peyer's patches are distinguished from surrounding ECs by their depressed position relative to the ECs, dark brush border, and short microvilli.

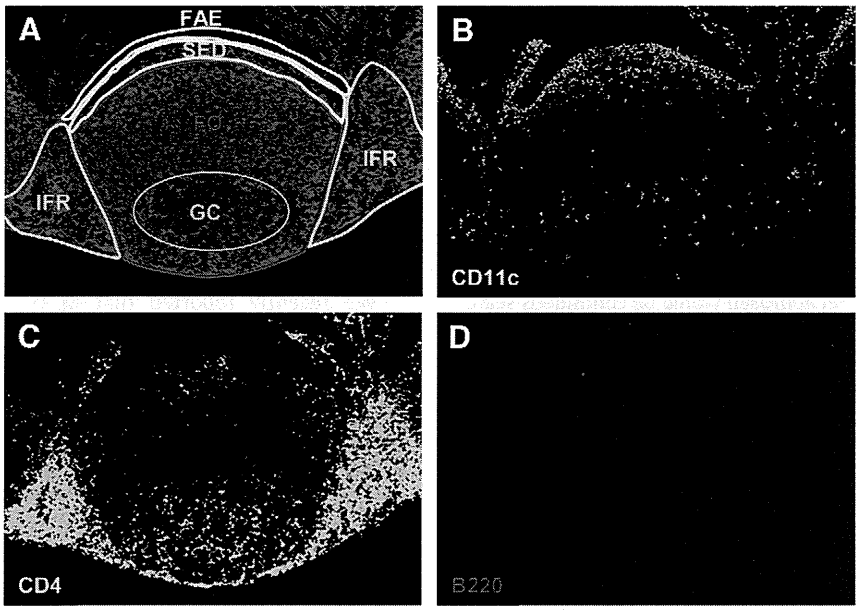

Fig. 3. Distinct cell distribution in the Peyer's patches. Immunohistochemical data on Peyer's patches is shown. (A) Each cell was identified with 4′,6-diamidino-2-phenylindole staining. PP compartments are outlined and labeled as follows: FO, follicle; FAE, follicle-associated epithelium; GC, germinal center; IFR, intrafollicular region; SED subepithelial dome. (B–D) Immunohistochemical staining of PPs for: dendritic cells (anti-CD11c; B), T cells (anti-CD4; C), B cells (anti-B220; D).

cellular environment for class switching of B cells from IgM to IgA (Fig. 3). Thus, PPs contain B cells at several differentiation and maturation stages: IgM^+B220^+ (~70%), $IgM^+IgA^+B220^+$ (~1%), IgA^+B220^+ (~3%), and IgA^+B220^- (~0.5%).

Approximately 20% of PP cells are T cells. Some portions of T cells are found in the IFRs of the PPs, which contain mainly naive T cells (Figs. 1 and 3) [11]. In addition to naïve T cells, other T cells exhibit active phenotype, including IFN-γ-producing Th1, IL-4-producing Th2, and IL-10-producing $Foxp3^+$ regulatory T cells [12]. A recent study demonstrated that at least some portions of $Foxp3^+$ regulatory T cells differentiated into follicular helper T cells which facilitate the B cell class switching to IgA^+ B cells in the GC [13].

Organogenesis of PPs is initiated in the embryonic stage. In mice, clustering of mesenchymal-lineage $VCAM\text{-}1^+ICAM\text{-}1^+$ PP organizer (PPo) cells starts at the site of tissue anlagen at embryonic days 14–16 [14]. PP inducer (PPi) cell are also key cells that initiate PP organogenesis. PPi cells are a component of lymphoid tissue inducer (LTi) cells that express key transcription factors, Id2 and RORγt, as well as a unique pattern of cell surface markers (IL-7 receptor [IL-7R]$^+$, $CD3^-$, $CD4^+$, $CD45^+$, lymphotoxin [LT] α1β2). The interaction between PPi and PPo cells through the IL-7R and LTβ receptors (LTβR) with corresponding cytokines results in production of lymphoid chemokines such as CXCL13 and CCL19/CCL21 from PPo cells. These chemokines recruit lymphocytes and DCs to form the PP micro-lymphoid structure. Several lines of evidence have demonstrated that the loss of any part of the organogenesis pathways results in the disruption or impairment of PP development [14]. Of note, disruption of the PP organogenesis pathway by blockade of IL-7R and/or LTβR signaling during a limited time period leads to the selective loss of PPs without affecting other lymphoid tissue organogenesis [14]. Experiments with PP-deficient mice showed that they failed to develop antigen-specific immune responses against orally administered particle-form antigens but retained their ability to respond to soluble forms of antigens [15,16], suggesting that PPs play an important role in the induction of antigen-specific immune responses against particulate antigen. The finding may provide a clue for the creation of mucosal antigen delivery vehicle which effectively distributes vaccine to appropriate intestinal inductive lymphoid tissues (e.g., GALT or PPs) covered by FAE containing M cells.

2.2. Isolated lymphoid follicles

Mice selectively deficient in PPs retain certain levels of intestinal IgA responses [15,16]; this finding demonstrates the presence of alternative induction pathways for intestinal IgA production that are independent of PPs. In fact, ILFs were identified as an additional inductive tissue for IgA production. ILFs are located throughout the small intestine as clusters of 100–200 lymphocytes [17]. As for PPs, the formation of ILFs is mediated by the crosstalk between LTi cells and organizer cells. Thus, ILF formation was impaired in RORγt-deficient mice, which lack both PPs and ILFs. When RORγt-deficient mice were reconstituted with $ROR\gamma t^+$ LTi, naturally produced intestinal IgA responses were recovered with the newly formed ILFs [18].

ILFs are composed of a single follicle that contains predominantly B cells and some DCs and are covered with a FAE, which contains M cells [17]. In contrast to PPs, ILFs lack T cell-rich IFRs. In agreement with this finding, a recent report indicated that ILFs are a site for T cell-independent IgA production. Indeed, in contrast to PPs, which lack the IgA^+ cells in T cell-deficient mice, many IgA^+ B cells were still noted in the ILFs of TCR-deficient mice [18]. For the delivery of vaccine antigen to the gut mucosal immune system, an interesting strategy might be the selective delivery of T cell-dependent and -independent antigens to PPs and ILFs, respectively.

3. Antigen-sampling system in the gut

3.1. M cells in the GALT are specialized for antigen sampling

As mentioned above, FAE in the PPs contains M cells that act as a portal for uptake of antigen from the intestinal lumen and transfer into the PPs [19]. Approximately 10% (mouse) and 5% (human) of cells in FAE are M cells [19]. In both mouse and humans, M cells have been shown to harboring some biological and immunological uniqueness that distinguishes them from surrounding ECs. For example, M cells are characterized by short microvilli, a thin glycocalyx, and reduced activity of intracellular lysosomes [19]. In addition, M cells exhibit an intra-pocket structure at basal sites, where lymphocytes and/or antigen-presenting cells including DCs locate. These features allow the M cells to easily take particle-form antigens including microorganisms from the

lumen and transport them into the PPs without digestion and processing [19]. M cells also show a unique glycosylation pattern. Thus, ulex europaeus (UEA-1) lectin binds α(1,2) fucose residues that are specifically expressed on mouse M cells and Goblet cells [20]. Similarly, sialyl Lewis A antigen recognized by specific antibody (LM112) is a potential candidate for an M cell marker in humans [21]. We recently developed a murine M cell-specific antibody (NKM 16-2-4) [22]. Intriguingly, the antibody also recognized α(1,2) fucose like UEA-1, but did not bind to Goblet cells that are recognized by UEA-1[20], indicating that additional unique glycosylation pattern exists in M cells. Thus, one interesting and novel approach would be continuous search and characterization of glycoprotein modification patterns of FAE cells for the development of glycosylation targeted vaccine delivery system.

In addition to physiological and morphological features, several receptors important for invasion of pathogens and/or uptake of luminal antigens have been identified on M cells. For example, β1 integrin, identified as a receptor for invasin-mediated infection by *Yersinia*, is expressed on M cells [23]. *Salmonella typhimurium* encodes the specific adhesion molecule, long polar fimbria, which targets M cells [24]. Reovirus derived protein σ1 binds to M cells [25]. Recently, glycoprotein 2 (gp2) was found to be expressed specifically on both human and murine M cells; it recognizes FimH, a component of type I pili on bacterial outer membranes, and thus gp2 acts as a receptor for FimH-expressing bacteria such as *Escherichia coli* and *S. Typhimurium* [26,27].

Several key pathways important in the development of M cells were also recently identified [28]. At the cellular level, studies in B cell-deficient mice suggest that B cells play an important role in the M cell development in PPs. B cell-deficient mice had a decreased number of M cells in PPs and adoptive transfer of B cells reversed this phenotype [29]. At the molecular level, the TNF superfamily plays a critical role in the development of M cells. A recent study demonstrated that CD137 (also known as 4-1BB and induced by lymphocyte activation [ILA]) is required for the functionality of M cells. CD137 deficiency thus resulted in a defect in particle transcytosis by M cells [30]. The fact that the ligand of CD137, 4-1BBL, is expressed on B cells and myeloid lineage cells may explain why M cell development is impaired in B cell-deficient mice. In addition to CD137, another TNF receptor superfamily member, receptor activator of nuclear factor κ-B ligand (RANKL), is reported to be involved in M cell differentiation. The number of M cells in FAE of PPs is reduced in mice lacking RANKL or treated with RANKL-specific neutralizing antibody [31]. These findings will likely yield novel strategies to enhance the M cell development and function, resulting in more efficient antigen delivery in the GALT. Thus, M cell development and function regulating molecules may become new generation of mucosal adjuvants for supporting and enhancing antigen-specific immune responses to orally administered vaccine.

3.2. Epithelial cells and villous M cells

Intestinal ECs not only act as a physiological barrier, but also take part in the immunological function of the intestine by the formation of secretary form of immunoglobulin leading to the secretion of IgA and IgM into the intestinal lumen [1]. Reciprocally, IgG, which is involved in the antigen transport system, is transported from the intestinal lumen via the neonatal Fc receptor (FcRn) expressed on the apical surface of ECs [32]. In addition, ECs release exosomes containing antigen bound to MHC class II. The released MHC-bound antigen is thought to induce tolerance, not activation, of antigen-specific T cell responses [33]. This system might be important aspect of the gut immune system for the creation of immunologically quiescence condition at the harsh environment of intestine.

Among ECs in the villous epithelium, we identified M cells sharing similar characteristic with the M cells originally found in the FAE of PPs (or PP M cells) and termed them villous M cells [34]. Villous M cells are thus morphologically similar to M cells in the PPs and are recognized by UEA-1 lectin and M cell-specific NKM16-2-4 antibody, a marker of murine M cells. The specificity for UAE-1 and NKM 16-2-4 antibody suggests that villous M cells most likely harbor identical α(1,2) fucose based glycosylation molecules. Like M cells, villous M cells were capable of taking up *Salmonella*, *Yersinia*, and *Escherichia coli* expressing invasin. In addition, they are found in villous epithelium in PP-deficient mice, which allow them to still induce antigen-specific IgA responses [15,16]. Thus, villous M cells are an alternative antigen-sampling site and can be consider as the additional targeting site for oral vaccine delivery.

We recently reported that M cell-like α(1,2) fucose based glycosylation can be induced on intestinal ECs by environmental stimuli such as colonization with commensal biota, treatment with cholera toxin, or treatment with dextran sodium sulfate and termed these cells as fucosylated ECs (F-ECs) [35]. Although a functional role of F-ECs in the induction of immune responses against intestinal antigens needs further investigation, these findings suggest additional possible strategies to induce F-ECs for the enrichment of antigen-sampling system at the intestinal epithelium to vaccine administered via oral route.

3.3. Intraepithelial DCs

It is also known that the gut immune system is full of antigen-presenting cells including different subsets of DCs [8]. Some DCs are observed in the epithelium of the terminal ileum, where they extend their dendrites into the lumen and thus capable of taking-up intestinal microorganisms. Among the several subsets of DCs, epithelial DCs uniquely express CX3CR1. They penetrate the epithelial layer without disrupting the epithelial barrier connected with highly sophisticated tight junction molecules such as occludin, claudin 1 and zonula occludens 1, and capture luminal bacteria [36,37]. Because of their unique histological positioning at intestinal epithelium, these DCs can be called as "intraepithelial DCs". Unlike other DCs, $CX3CR1^+$ intraepithelial DCs are a non-migratory and gut-resident population, suggesting that the $CX3CR1^+$ population might play a critical role in the initiation or modulation of local immune responses in the intestinal epithelium or lamina propria regions [38]. Thus, these $CX3CR1^+$ DCs resided in the intestinal epithelium could also be useful targeted cell population for oral vaccine delivery.

4. Induction and regulation of IgA-mediated immune responses in the gut

4.1. GALT-mediated induction of IgA responses

A highly integrated sequence of processes of cellular and molecular interaction occurs in the PPs that lead to the initiation of antigen-specific immune responses (Fig. 4). Antigen transport from intestinal lumen by M cells at the FAE of PPs is an initial step for the induction of antigen-specific immune responses after oral immunization. Antigen is then taken up by DCs that are localized in the pocket of M cells or underneath M cells. Resultant up-regulation of CCR7 chemokine receptor expression on the DCs, allows them to move to the T cell region via locally produced corresponding chemokines (CCL19 and CCL21) in the PP or mesenteric lymph nodes and then present the processed peptide antigen for the generation of antigen-specific T cells [39].

Antigen-primed T cells support IgA class switching and somatic hyper mutation of B cells in the GC through antigen-specific interactions, CD40/CD40 ligand interaction, and cytokine expression (e.g., TGF-β, IL-4, and IL-21) [5]. Simultaneously, retinoic acid derived from PP DCs induces the expression on primed T and B cells of the gut-imprinting molecules α4β7 integrin and CCR9 [9,10]. B cells also alter their expression of receptors for other chemokines (e.g., CXCR5 and CCR10) and sphingosine 1-phosphate, thus determining whether they